"Astronomy and Dynamics", International Workshop
in honor of Jacques Laskar April 28-30, 2015
Observatoire de Paris

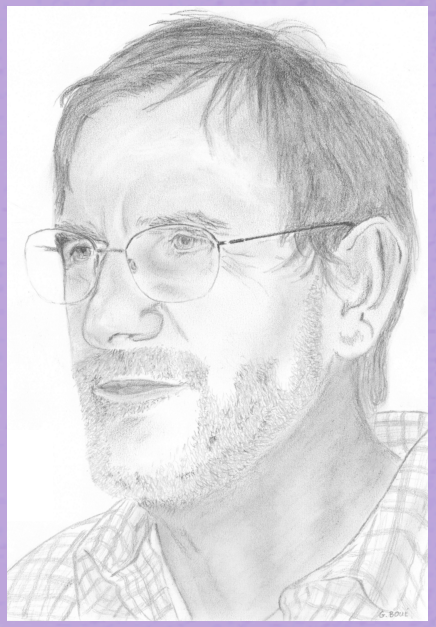

# From Galaxies to Accelerators through Frequency Map Analysis

Yannis PAPAPHILIPPOU, CERN

28/04/2015

# Galactic dynamics

- Main purpose to reconcile morphology and kinematics
  - N-body simulations
  - Mean potential
- Use dynamical system methods to study dynamics of triaxial galactic models

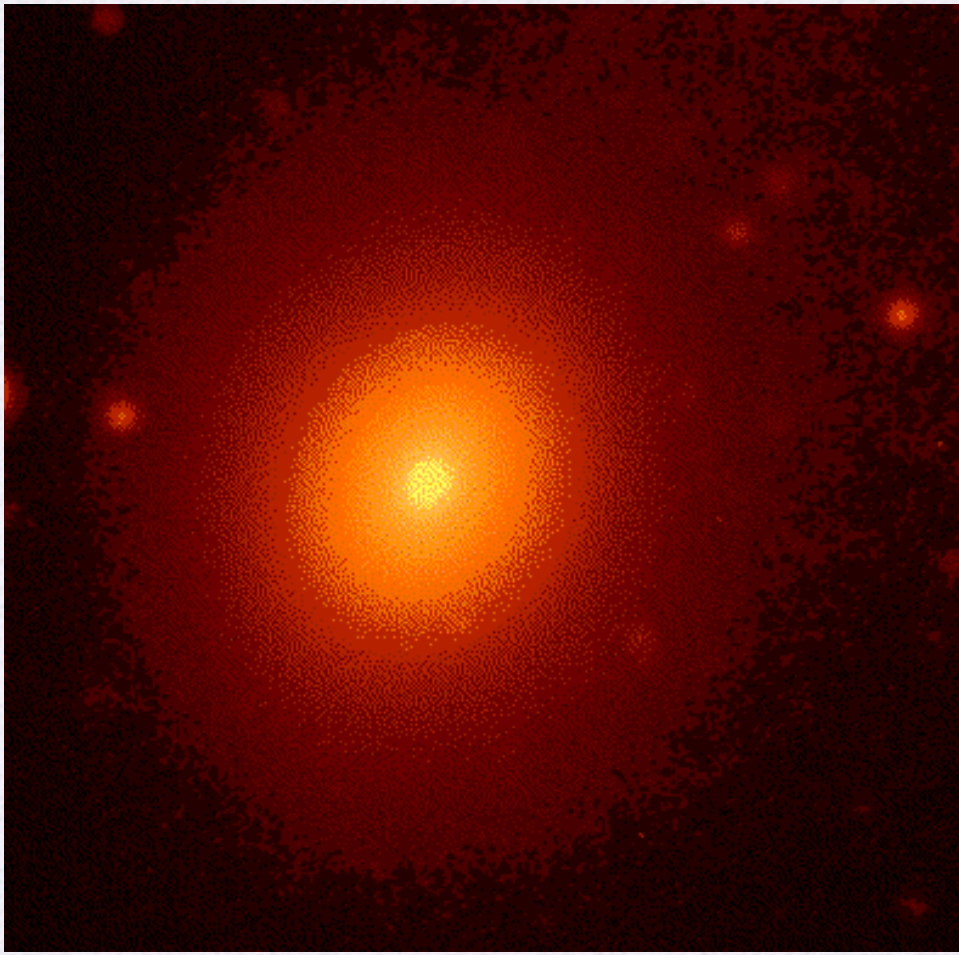

# The logarithmic potential

J. Binney, MNRAS, 196, 1981

- Flat rotation curve of spiral galaxies (massive haloes)
- Ellipsoidal equipotential (elliptical galaxies)
- Density function $\rho \propto R^{-2}$

$$H = \frac{1}{2}(X^2 + Y^2 + Z^2) + \ln(x^2 + \frac{y^2}{q_1^2} + \frac{z^2}{q_2^2} + R_c^2)$$

  - $(x, y, z)$ positions and $(X, Y, Z)$ conjugate momenta
  - $q_1,\ q_2$ axial ratios (perturbation parameters)
  - $R_c$ radius of a central bulge (regularisation parameter)
- Integrable cases
  - 1 deg. of freedom on invariant planes $(x, X),\ (y, Y),\ (z, Z)$
  - 2 degrees of freedom "central" systems $(q_1 = 1, z = Z = 0)$, $(q_2 = 1, y = Y = 0),\ (q_1 = q_2, x = X = 0)$
  - 3 degrees of freedom "spherical" systems $q_1 = q_2 = 1$

# Frequency map analysis

- Frequency Map Analysis (FMA) is a numerical method which springs from the studies of J. Laskar putting in evidence the chaotic motion in the Solar Systems
- FMA was successively applied to several dynamical systems
  - Celestial mechanics J.Laskar and P.Robutel, Nature 361, 608, 1993
  - 4D maps J.Laskar, Physica D 67, 257–281, 1993
  - Galactic Dynamics Y.P. and J.Laskar, A&A, 307, 427, 1996<br>Y.P. and J.Laskar, A&A, 329, 451, 1998
  - Accelerator beam dynamics: lepton and hadron rings

H.S.Dumas and J.Laskar, PRL 70, 2975, 1993
J.Laskar and D.Robin, Part.Accel. 54, 183, 1996
Y.P, PAC99, 1554, 1999
L.Nadolski and J.Laskar, PRSTAB 6, 114801, 2003
**Y.P., Chaos, 24, 024412, 2014**

# Frequency Map Analysis: in a nutshell

J. Laskar, A&A, 1988, Icarus, 1990

Quasi-periodic approximation through **NAFF** algorithm $f'_j(t) = \sum_{k=1}^{N} a_{j,k} e^{i\omega_{j,k} t}$

of a complex phase space function $f_j(t) = q_j(t) + ip_j(t)$ defined over $t = \tau$

for each degree of freedom $j = 1, \ldots, n$ with $\omega_{j,k} = \boldsymbol{k}_j \cdot \boldsymbol{\omega}$

and $a_{j,k} = A_{j,k} e^{i\phi_{j,k}}$

**Advantages of NAFF**:

a) Very accurate representation of the "signal" $f_j(t)$ (if quasi-periodic) and thus of the amplitudes

b) Determination of frequency vector $\boldsymbol{\omega} = 2\pi\boldsymbol{\nu} = 2\pi(\nu_1, \nu_2, \ldots, \nu_n)$

with high precision $\longrightarrow \frac{1}{\tau^4}$ for Hanning Filter

# Aspects of the frequency map

- In the vicinity of a resonance the system behaves like a pendulum
- Passing through the elliptic point for a fixed angle, a fixed frequency (or rotation number) is observed
- Passing through the hyperbolic point, a frequency jump is observed

$$F : \mathbb{B}^n \longrightarrow \mathbb{R}^n$$
$$(I) \longrightarrow (\nu)$$

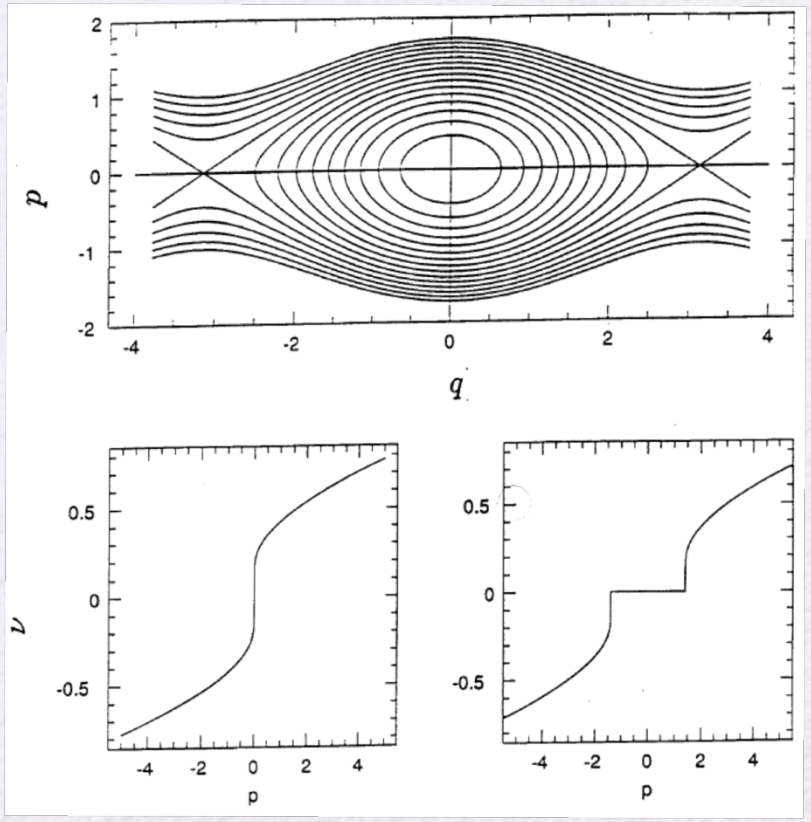


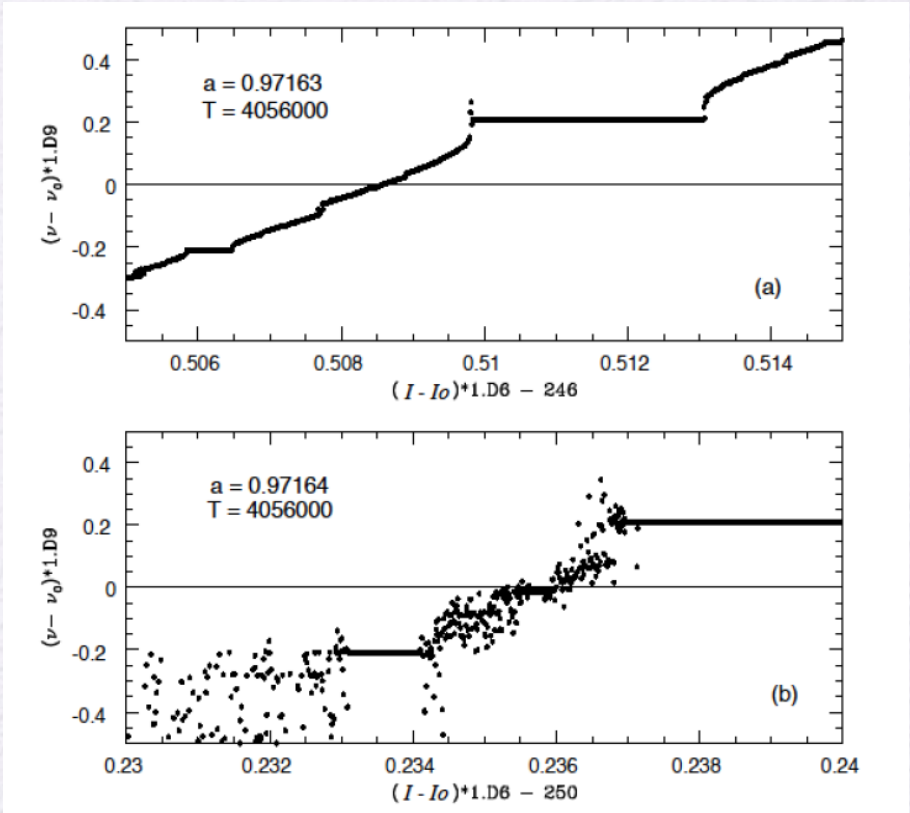

# The planar logarithmic potential

$$H = \frac{1}{2}(X^2 + Y^2) + \ln(x^2 + \frac{y^2}{q^2} + R_c^2)$$

Y.P. and J.Laskar, A&A, 307, 427, 1996

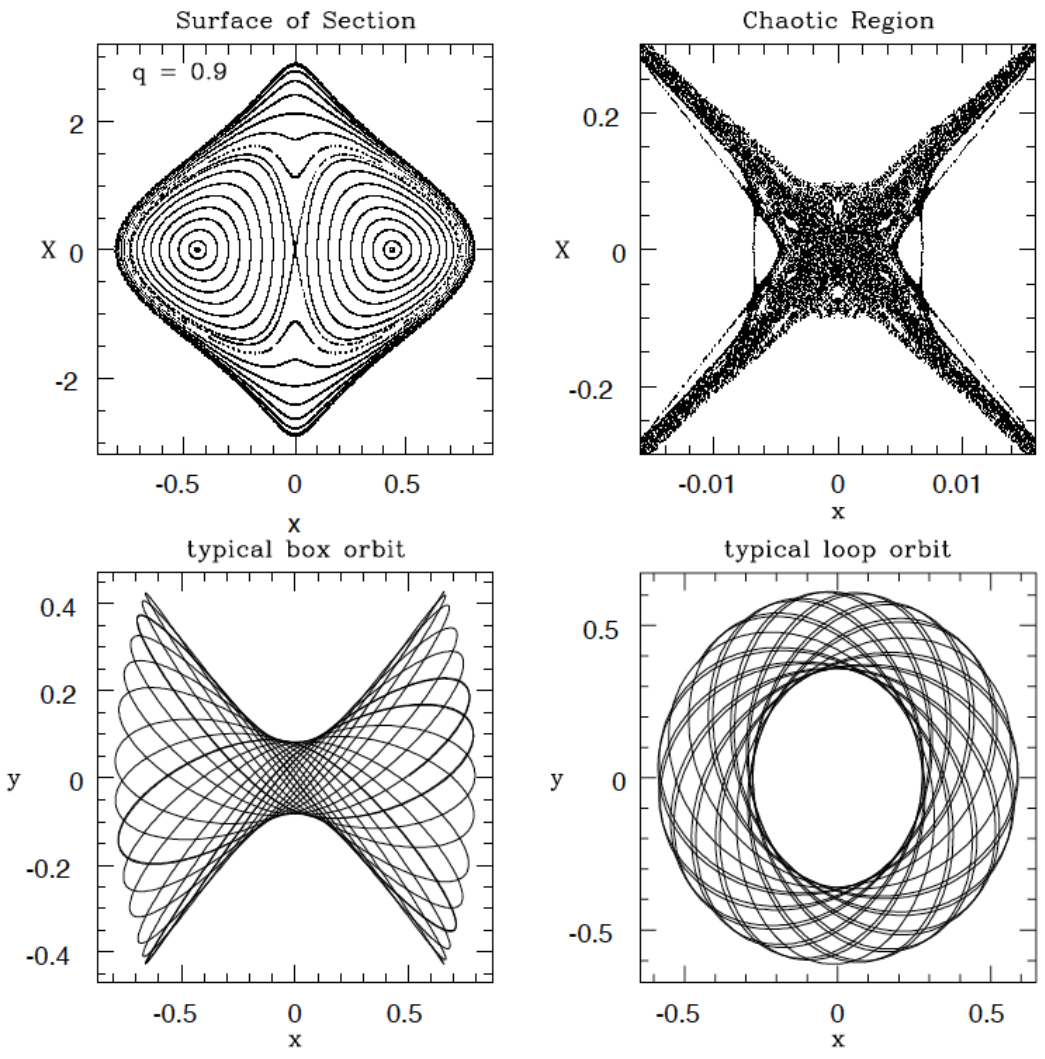

# Frequency maps for the planar logarithmic potential

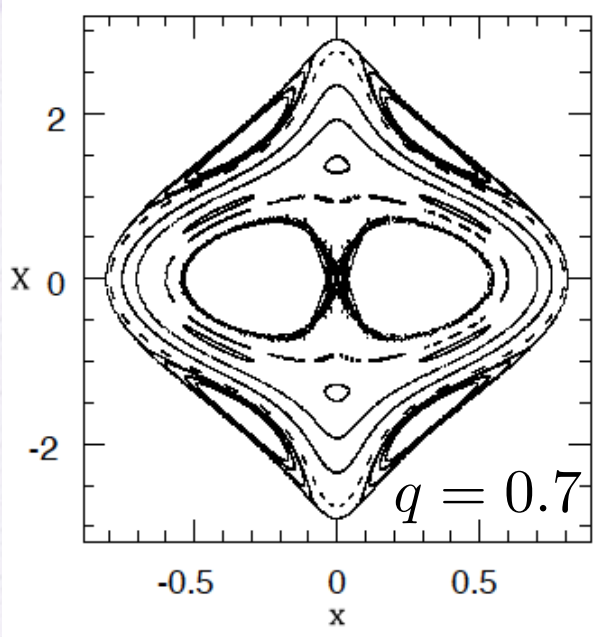


$$F_{\mathcal{B}} : (0, X_{max}) \longrightarrow \mathbb{R}$$

$$X \longrightarrow \frac{\nu_x}{\nu_y}$$

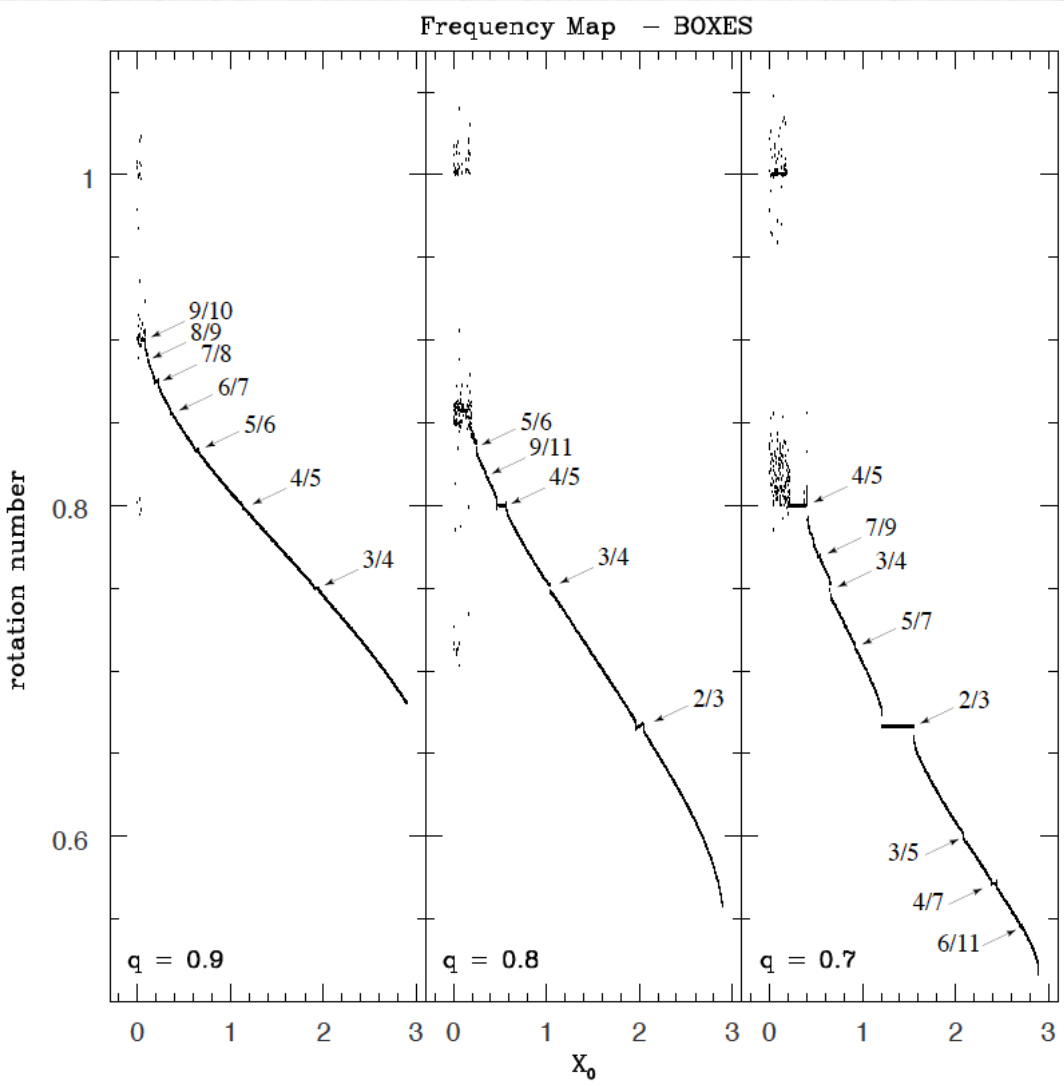

# Orbits in the 3D logarithmic potential

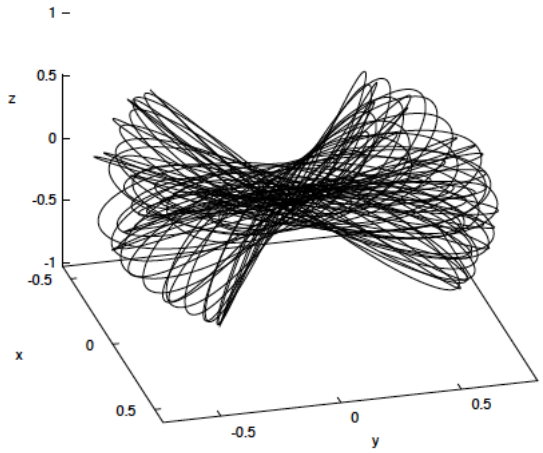


"Boxes"

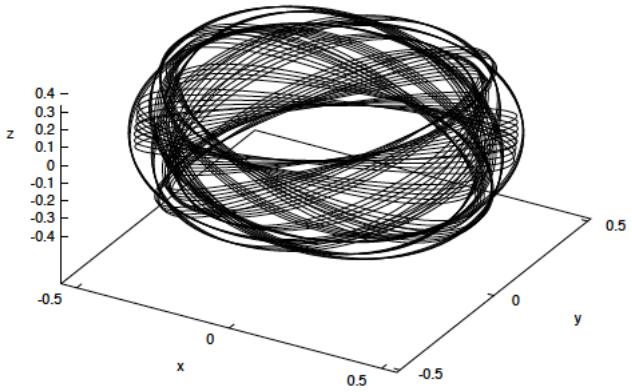


"small-axis Tubes"

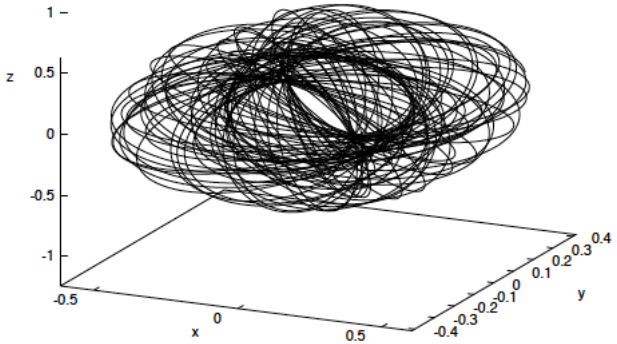


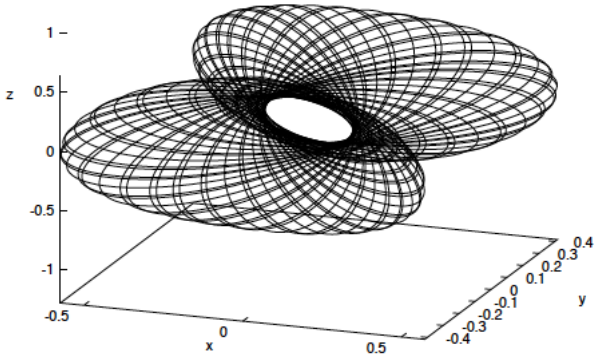


"outer" and "inner long axis Tubes"

# Frequency maps for the 3D logarithmic potential

Y.P. and J.Laskar, A&A, 329, 451, 1998

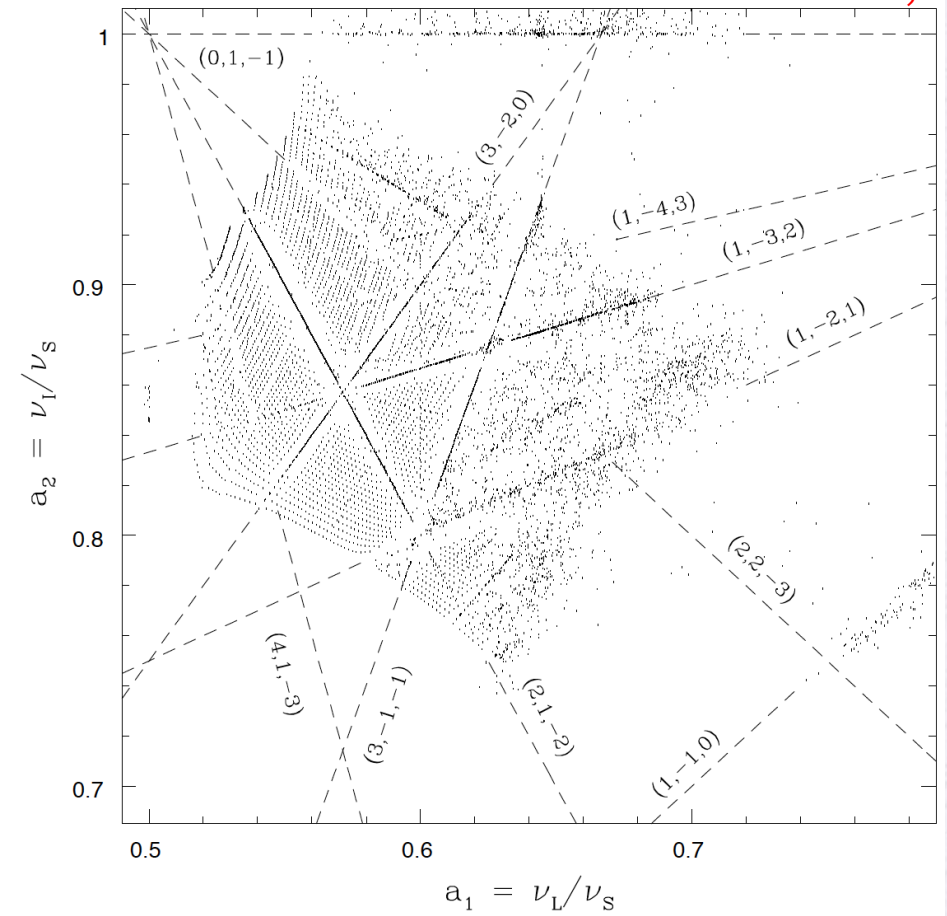


$q_1 = 1.25, q_2 = 0.9$

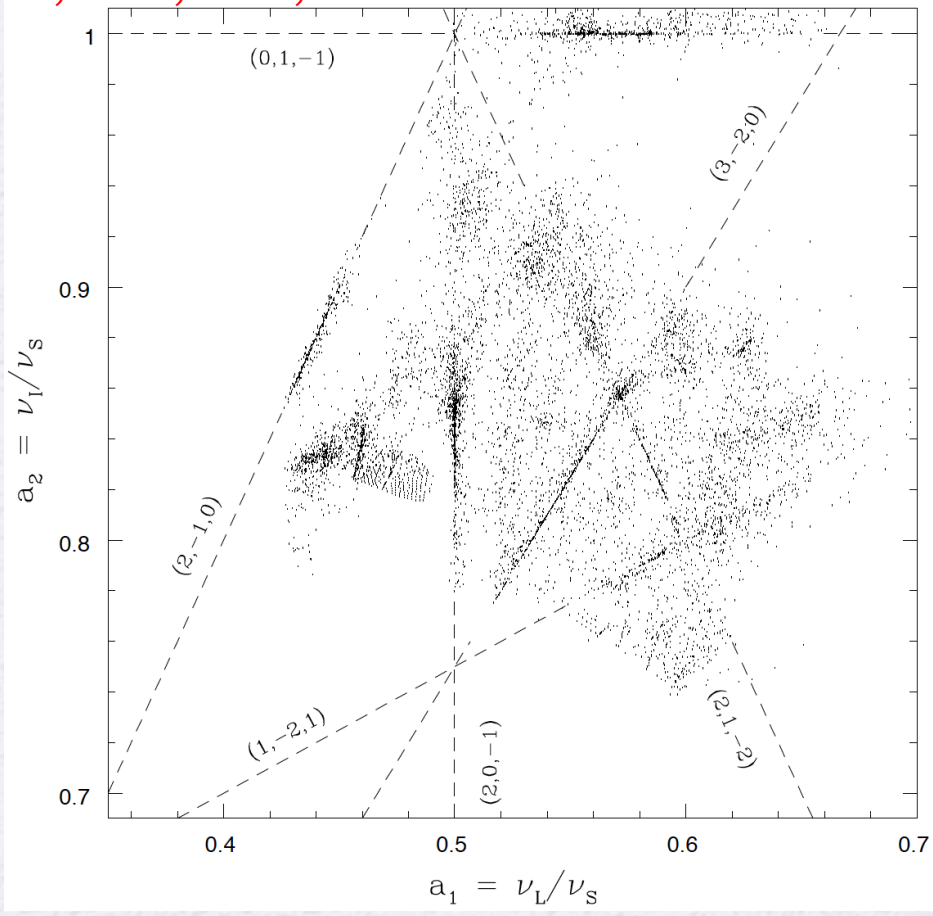


$q_1 = 1.5, q_2 = 0.9$

# Frequency analysis for orbit classification

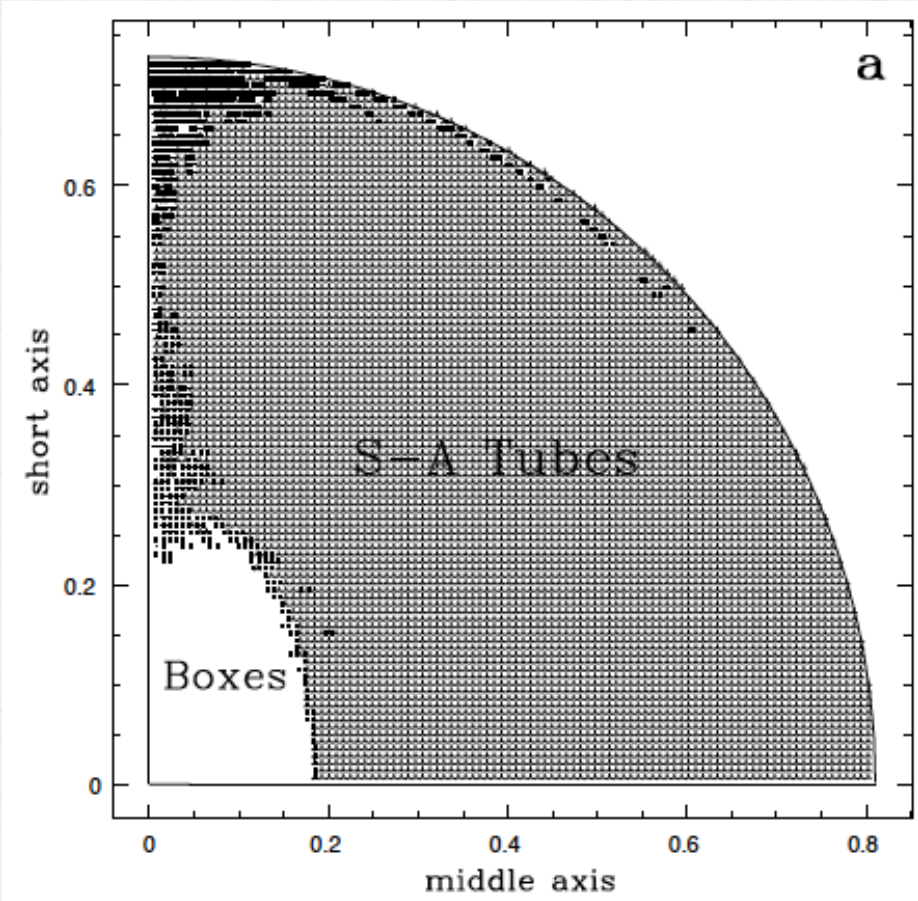


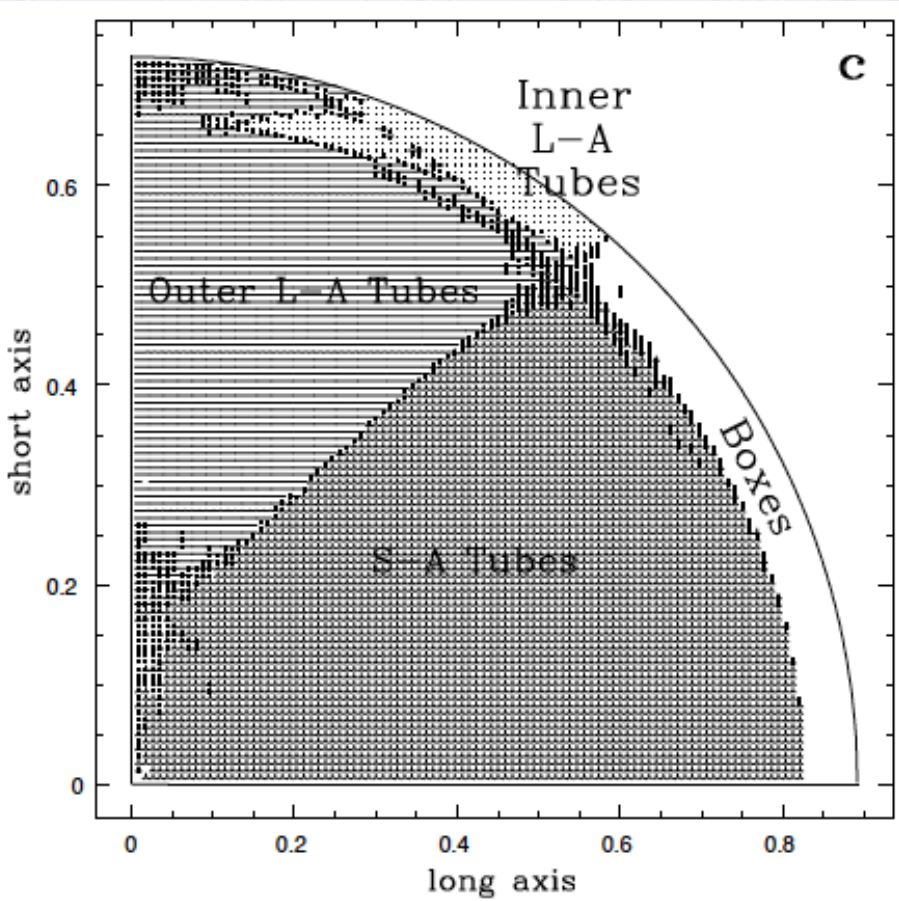


$$q_1 = 1.1, q_2 = 0.9$$

# Frequency analysis for orbit classification

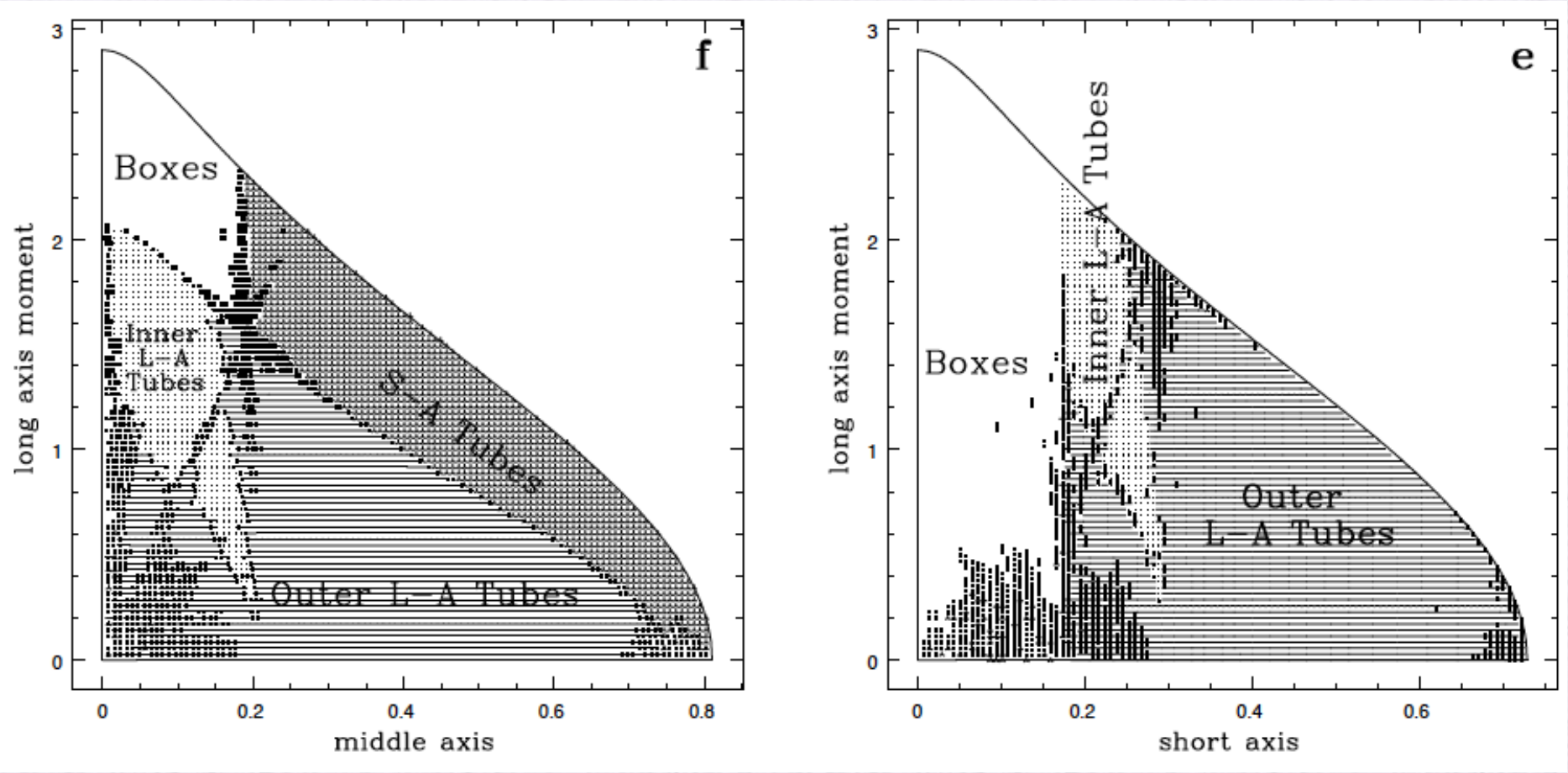


$$q_1 = 1.1, q_2 = 0.9$$

# In conclusion…

- Dynamical aspects of triaxial galactic models
  - Resonant tori (Periodic orbits in physical space)
  - Regular and chaotic regions
  - Importance of rectilinear periodic orbits
- Existence of large chaotic regions
- Necessity of including chaotic orbits for the construction of galactic models
- Further confirmed with **exactly** the same approach in different galactic models

M. Valluri, D. Merritt, ApJ, 1998, 1999
F.C. Wachlin, S. Ferraz-Mello, MNRAS, 1998

# From the infinitesimally large…

# …to the infinitesimally small…

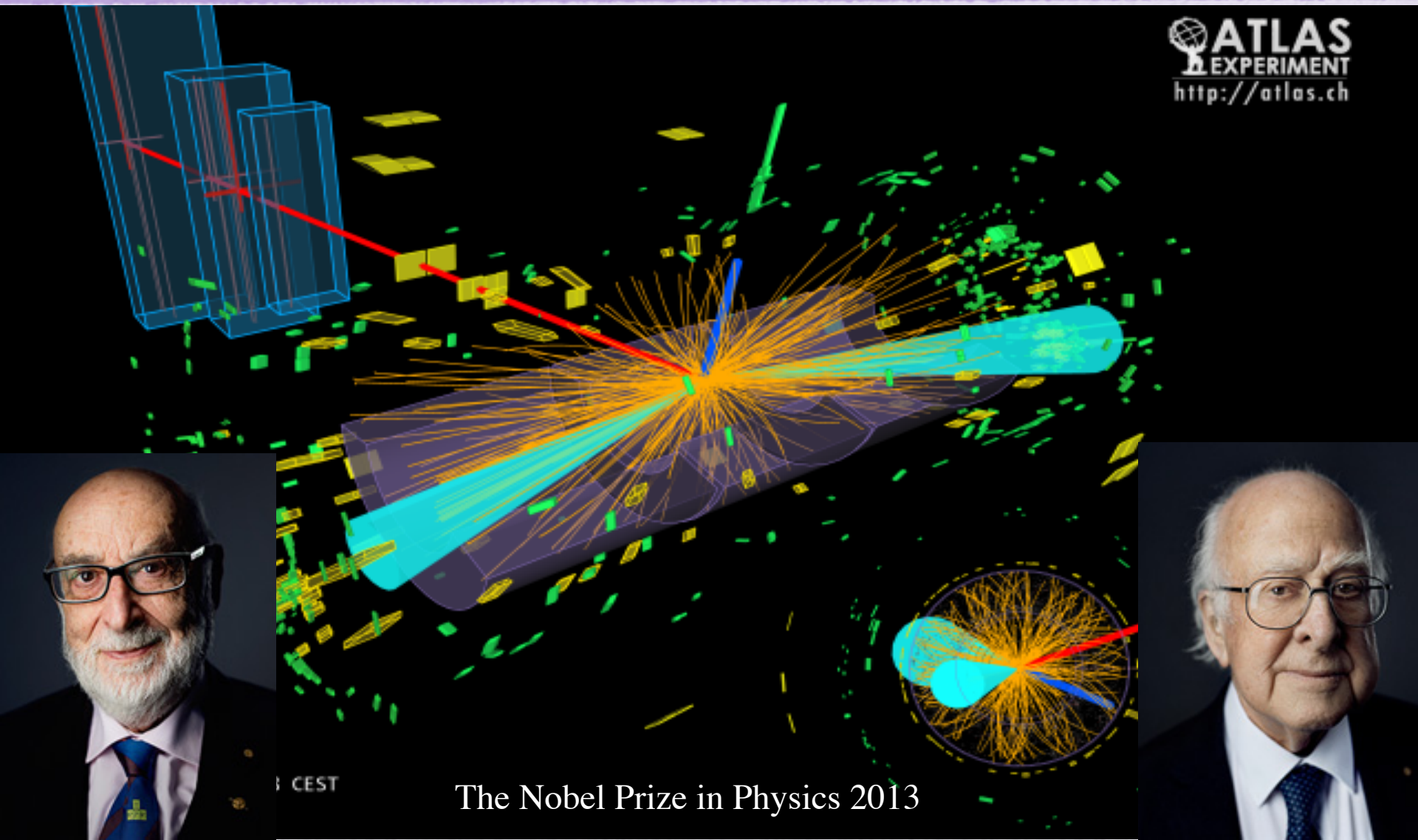


The Nobel Prize in Physics 2013

# …through frequency map analysis

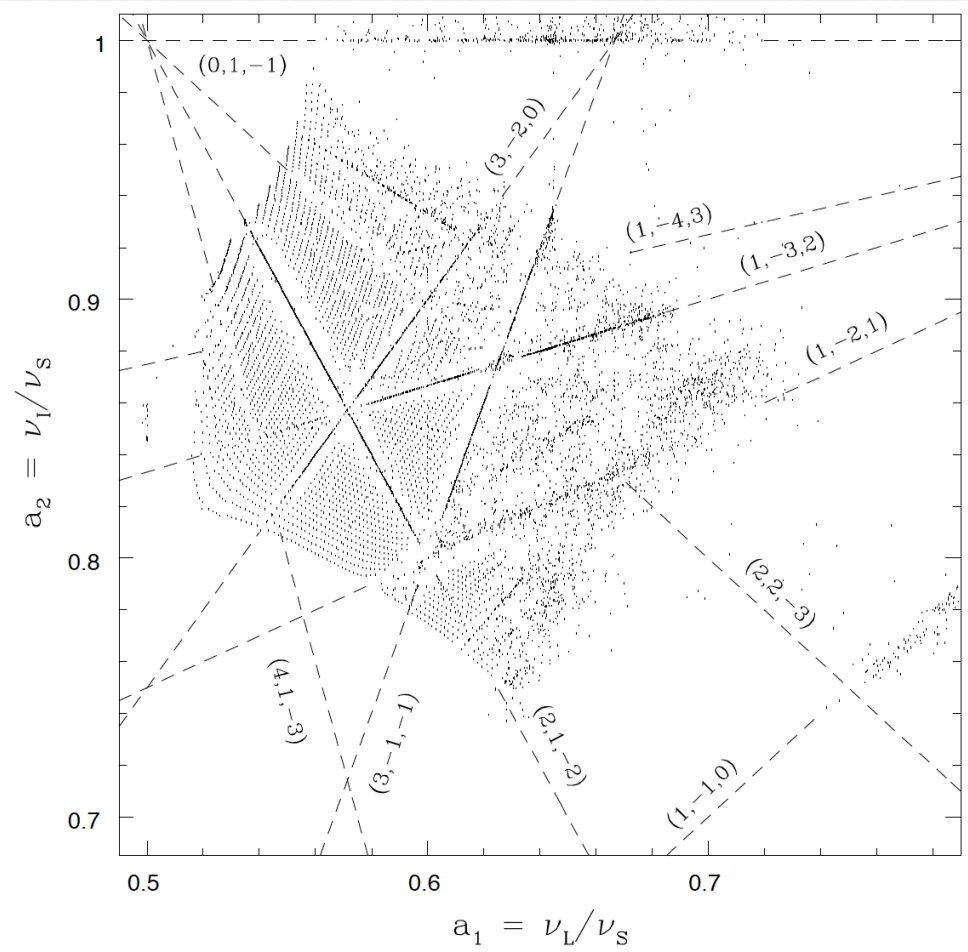


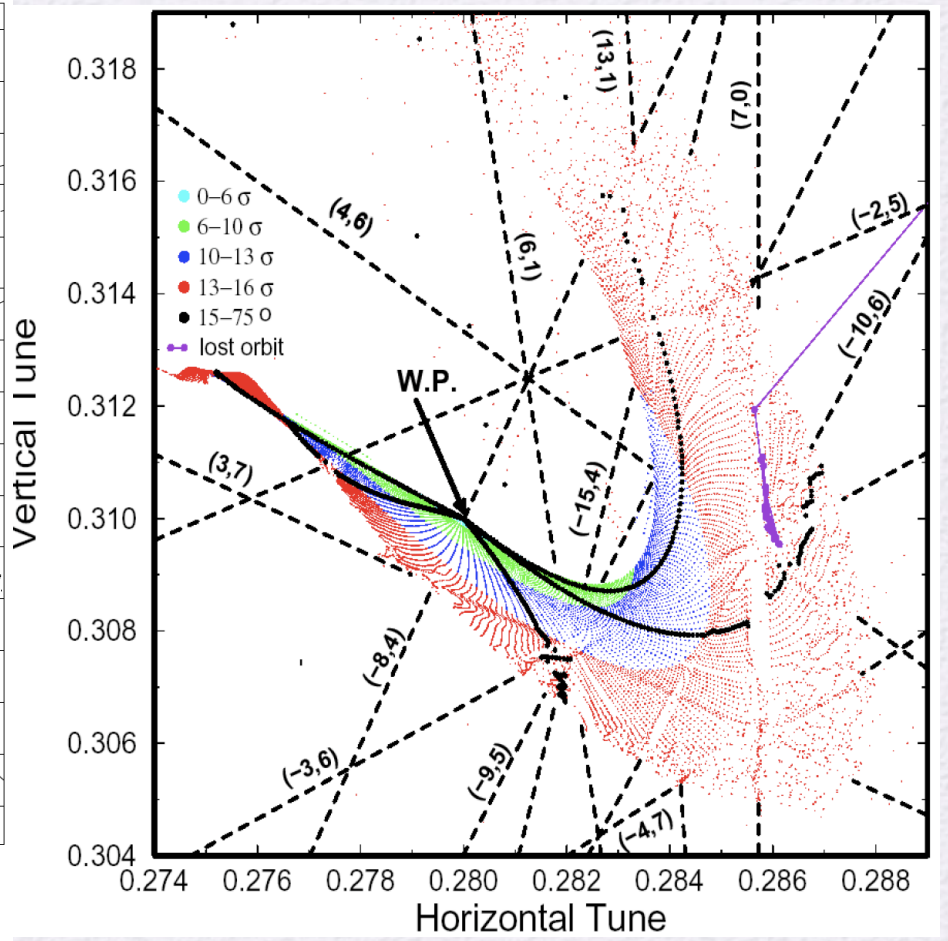


Galactic model

The LHC

# Non-linear effects in accelerators


- Non-linear magnets (sextupoles, octupoles)
- Magnet imperfections and misalignments
- Noise (power supply ripple, ground motion)
- Insertion quadrupoles
- Magnets in experimental areas (solenoids, dipoles)
- Injection elements
- Magnet fringe fields
- Insertion devices (wigglers, undulators)
- Beam-beam effect (head on and long range)
- Space-charge effect
- Electron cloud (Ion) effects

- Performance issues
  - Particle losses causing
    - Reduced lifetime
    - Radio-activation (super-conducting magnet quench)
    - Reduced machine availability
  - Beam size blow-up
  - Reduced number of bunches and/or increased crossing angle
  - Reduced intensity
- Cost issues
  - Number of magnet correctors and families (power convertors)
  - Magnetic field and alignment tolerances

# Single-particle relativistic Hamiltonian

- Neglecting self fields and radiation, motion can be described by a single-particle Hamiltonian

$$H(\mathbf{x},\mathbf{p},t) = c\sqrt{\left(\mathbf{p} - \frac{e}{c}\mathbf{A}(\mathbf{x},t)\right)^2 + m^2c^2} + e\Phi(\mathbf{x},t)$$

  - $\mathbf{x} = (x, y, z)$ Cartesian positions
  - $\mathbf{p} = (p_x, p_y, p_z)$ conjugate momenta
  - $\mathbf{A} = (A_x, A_y, A_z)$ the magnetic vector potential
  - $\Phi$ the electric scalar potential
- The ordinary kinetic momentum vector is written as

$$\mathbf{P} = \gamma m\mathbf{v} = \mathbf{p} - \frac{e}{c}\mathbf{A}$$

with $\mathbf{v}$ the velocity vector and $\gamma = (1 - v^2/c^2)^{-1/2}$ the relativistic factor

# Accelerator Hamiltonian

- Introduce **approximations**
  - Neglect electric potential (decouple longitudinal motion from transverse)
  - Consider only static transverse magnetic fields, so vector potential with only longitudinal component

$$A_s(x,y,s) = \left(1 + \frac{x}{\rho(s)}\right) B_0 \Re e \sum_{n=0}^{\infty} \frac{b'_n(s) - i a'_n(s)}{n+1} (x+iy)^{n+1}$$

  - Consider total momentum much higher than transverse (true for high-energy) and expand the square root to 1st order
  - Impose that radius of curvature $\rho(s)$ is much larger than transverse position (large ring approximation)
- Apply **canonical transformations**, by first setting the independent variable as the path length $s$ and move the periodic orbit to the origin

$$\mathcal{H} = \frac{p_x^2 + p_y^2}{2(1+\delta)} - \frac{x(1+\delta)}{\rho(s)} - e\hat{A}_s \quad \text{with} \quad \delta \equiv \frac{P_t - P_0}{P_0}$$

# Classical perturbation theory

- It is convenient to separate Hamiltonian to an integrable part plus a perturbation

$$\mathcal{H}(x, y, p_x, p_y, s) = \mathcal{H}_0(x, y, p_x, p_y, s) + \sum_{k_x, k_y} h_{k_x, k_y}(s) x^{k_x} y^{k_y}$$

where the polynomial coefficients are periodic $h_{k_x,k_y}(s) = h_{k_x,k_y}(s + C)$

- Integrable Hamiltonian derived by considering only dipole (uniform) fields, normal quadrupole (linear) magnetic fields, with normalized gradient $K(s)$

$$\mathcal{H}_0 = \frac{p_x^2 + p_y^2}{2(1+\delta)} - \frac{x\delta}{\rho(s)} + \frac{x^2}{2\rho(s)^2} + \frac{K(s)}{2}(x^2 - y^2)$$

- Classical perturbation theory already applied in the early days of the first synchrotrons for analyzing non-linear part (resonance driving terms)

J. Moser, CERN Symp, HEACC, 1956;
R. Hagedorn, CERN Yellow Report 57-1, 1957;
A. Shoch, CERN Yellow Report, 57-21, 1958

# Accelerator Maps

A.J. Dragt and J.M. Finn, J. Math. Phys. 17, 2215, 1976;
A.J. Dragt, IEEE Trans. Nucl. Sc., NS-26, No. 3, 3601,1979

- Lie formalism introduced for representing symplectic accelerator maps
- For a Hamiltonian system $H(\mathbf{z},t)$, a formal solution of the equations of motion $\frac{d\mathbf{z}}{dt} = [H,\mathbf{z}] =: H : \mathbf{z}$, is written as

  $\mathbf{z}(t) = \sum_{k=0}^{\infty} \frac{t^k :H:^k}{k!}\mathbf{z}_0 = e^{t:H:}\mathbf{z}_0$ , with $\mathcal{M} = e^{:H:}$ a symplectic map
- The 1-turn accelerator map represented by composition of maps of each element $\mathcal{M} = e^{:f_2:}\ e^{:f_3:}\ e^{:f_4:}\ \ldots$
- Differential algebra tools used for computing efficiently the map
- Normal form approaches applied to the numerically constructed map

E. Forest, M. Berz, and J. Irwin, PA, 24, 91, 1989;
M. Berz, PA, 24, 109, 1989;
A. Bazzani, G. Servizi, E. Todesco, and G. Turchetti, CERN Yellow Report, 94-02, 1994.

# Normal form analysis of LHC models

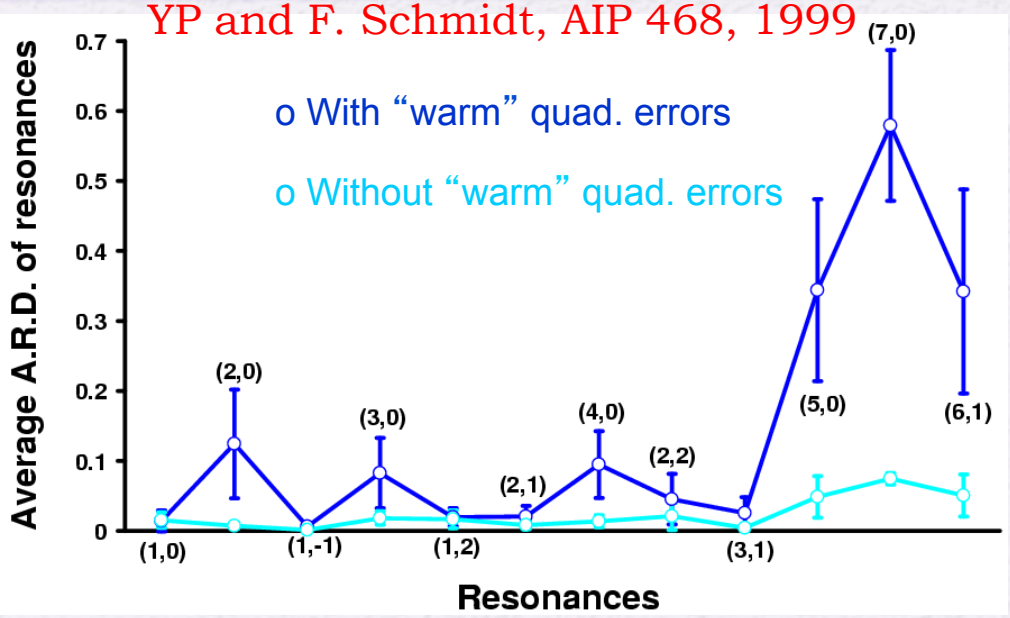


| Phase | Type | DA ($\sigma$) | LHC Version | | |
|---|---|---|---|---|---|
| | | | 4 | 5 | |
| | | | | Nominal | Target |
| 15° | Warm Quads switched ON | Average | 10.0 | 9.1 | 10.4 |
| | | Minimum | 8.5 | 7.4 | 8.6 |
| | Warm Quads switched OFF | Average | 10.7 | 11.5 | 12.4 |
| | | Minimum | 9.6 | 10.3 | 11.3 |
| 45° | Warm Quads switched ON | Average | 11.1 | 11.3 | 12.8 |
| | | Minimum | 9.5 | 9.2 | 11.4 |
| | Warm Quads switched OFF | Average | 11.4 | 12.4 | 13.8 |
| | | Minimum | 10.1 | 10.7 | 12.3 |

- Long term stability ($10^7$ turns) of LHC @ injection affected from random imperfections mainly in the super-conducting (dipole) magnets
- Area of stability (**Dynamic aperture** - DA) computed with particle tracking for random magnet error distributions
- Numerical tool based on normal form analysis (GRR) permitted identification of the reason for DA reduction between the "old" and an improved version of the LHC optics (errors in the "warm" quadrupoles)

# Chaos detection methods in particle accelerators

- Computing/measuring dynamic aperture (DA) or particle survival

  A. Chao et al., PRL 61, 24, 2752, 1988;
  F. Willeke, PAC95, 24, 109, 1989.

- Computation of Lyapunov exponents

  F. Schmidt, F. Willeke and F. Zimmermann, PA, 35, 249, 1991;
  M. Giovannozi, W. Scandale and E. Todesco, PA 56, 195, 1997

- Variance of unperturbed action (a la Chirikov)

  B. Chirikov, J. Ford and F. Vivaldi, AIP CP-57, 323, 1979
  J. Tennyson, SSC-155, 1988;
  J. Irwin, SSC-233, 1989

- Fokker-Planck diffusion coefficient in actions

  T. Sen and J.A. Elisson, PRL 77, 1051, 1996

- **Frequency map analysis**

# Frequency maps for the LHC

Y.P., PAC1999

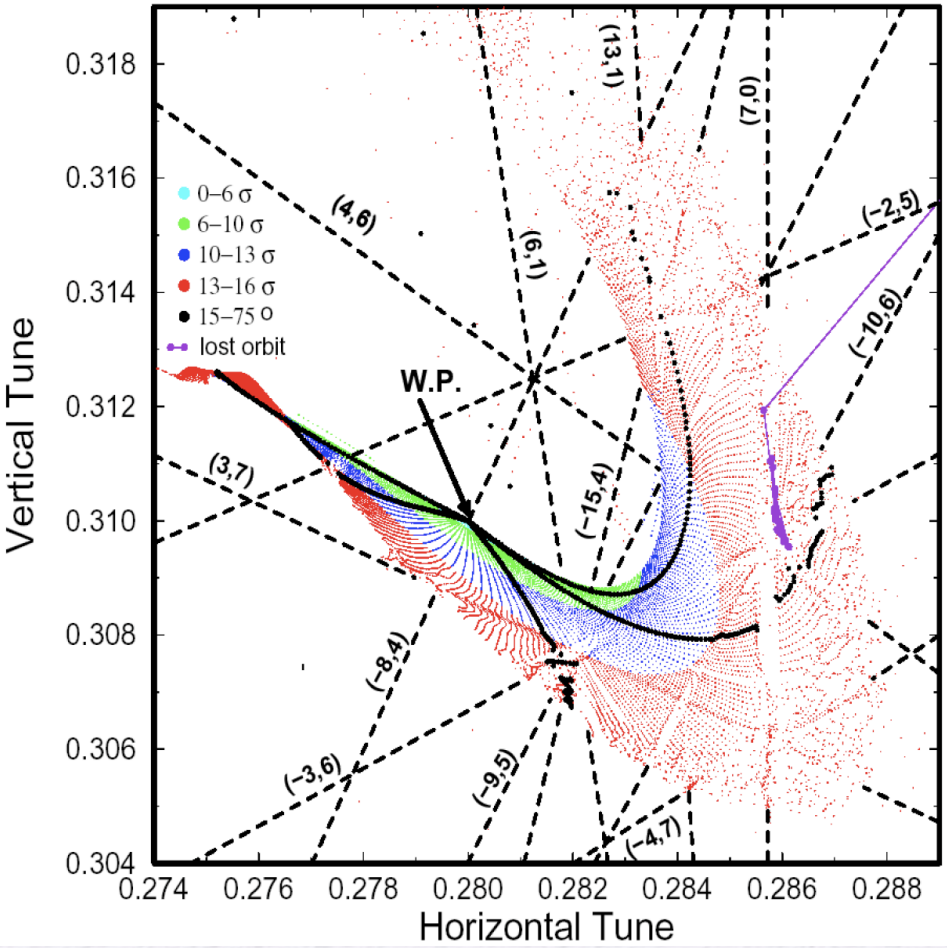


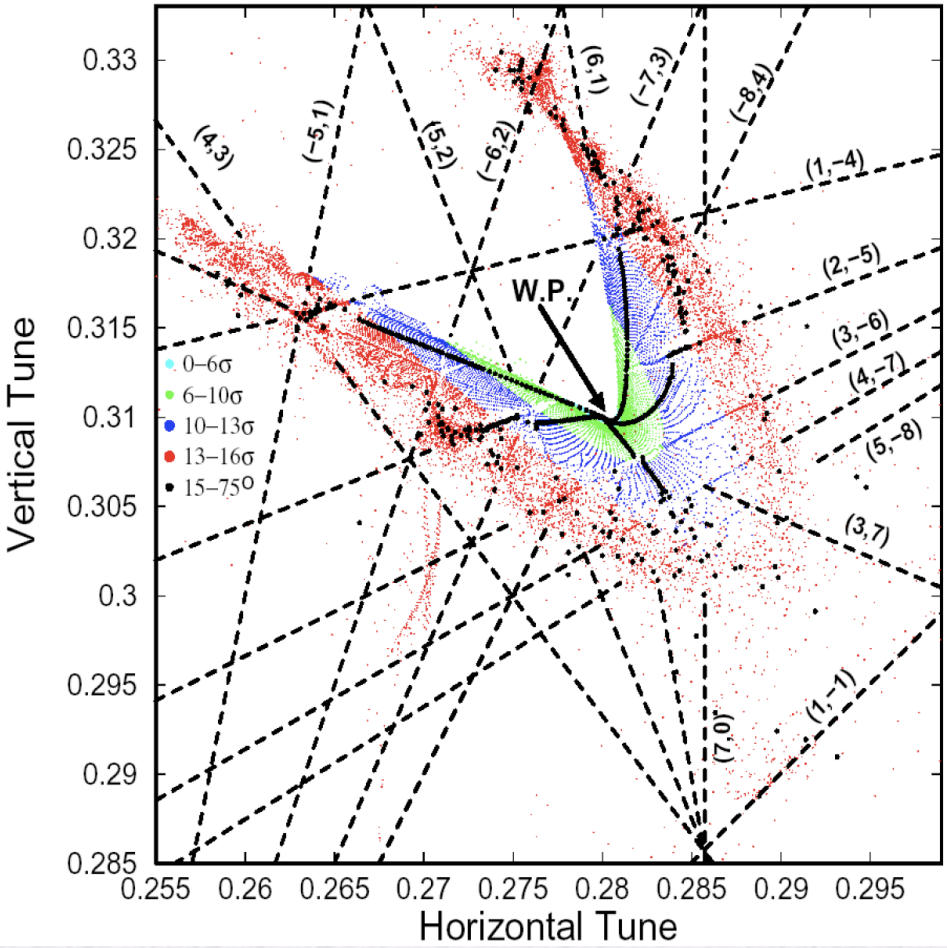


Frequency maps for the target error table (left) and an increased random skew octupole error in the super-conducting dipoles (right)

# Diffusion Maps

J. Laskar, PhysicaD, 1993

- Calculate frequencies for two equal and successive time spans and compute frequency diffusion vector:

$$\boldsymbol{D}|_{t=\tau} = \boldsymbol{\nu}|_{t\in(0,\tau/2]} - \boldsymbol{\nu}|_{t\in(\tau/2,\tau]}$$

- Plot the initial condition space color-coded with the norm of the diffusion vector
- Compute a diffusion quality factor by averaging all diffusion coefficients normalized with the initial conditions radius

$$D_{QF} = \left\langle \frac{|\boldsymbol{D}|}{(I_{x0}^2 + I_{y0}^2)^{1/2}} \right\rangle_R$$

# Diffusion maps for the LHC

Y. P., PAC1999

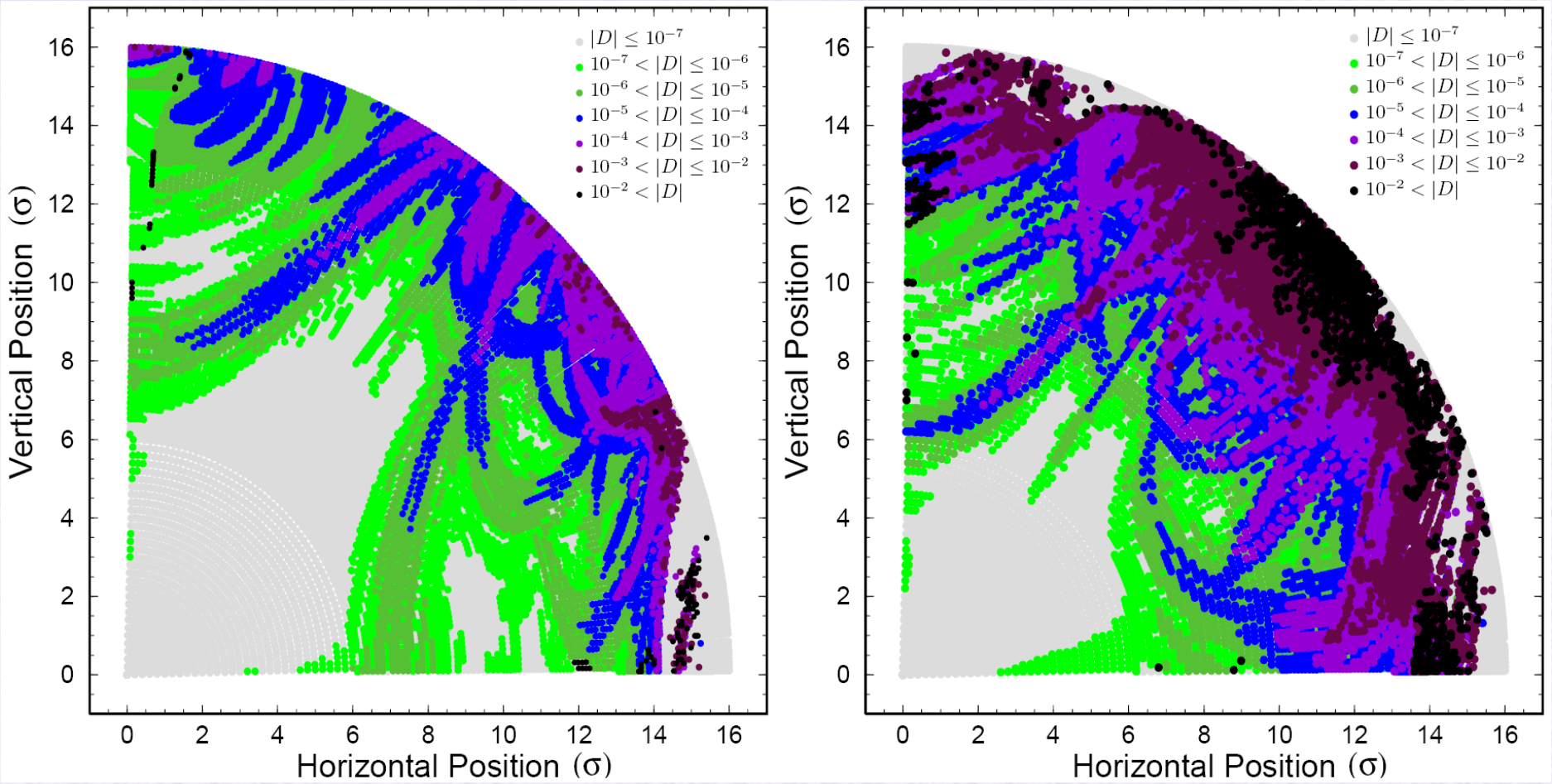


Diffusion maps for the target error table (left) and an increased random skew octupole error in the super-conducting dipoles (right)

# Correction schemes efficiency

Y. P., EPAC2000

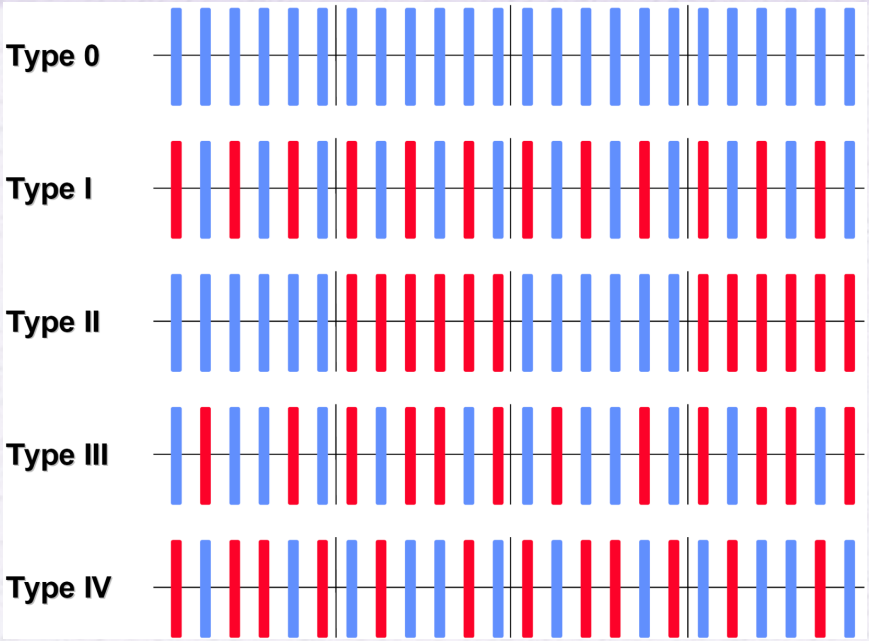


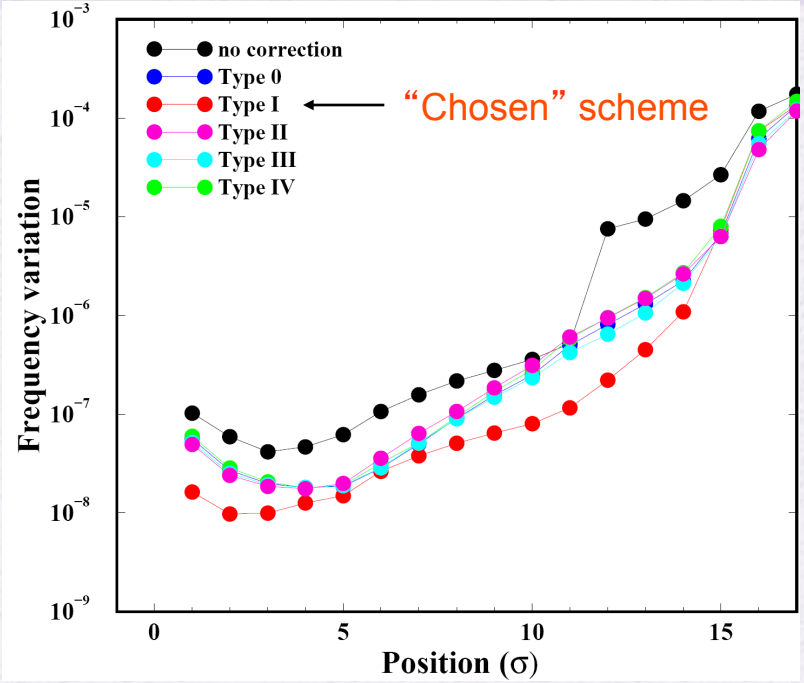


- Comparison of correction schemes for $b_4$ and $b_5$ errors in the LHC dipoles
- Frequency maps, resonance analysis, tune diffusion estimates, survival plots and short term tracking, proved that only half of the correctors are needed

# Magnet fringe fields

Y. P. and D.T. Abell, EPAC2000

- From the hard-edge Hamiltonian

$$H_f = \frac{\pm Q}{12B\rho(1+\frac{\delta p}{p})}(y^3p_y - x^3p_x + 3x^2yp_y - 3y^2xp_x),$$

the first order shift of the frequencies with amplitude can be computed analytically

$$\begin{pmatrix}\delta\nu_x\\ \delta\nu_y\end{pmatrix} = \begin{pmatrix}a_{hh} & a_{hv}\\ a_{hv} & a_{vv}\end{pmatrix}\begin{pmatrix}2J_x\\ 2J_y\end{pmatrix},$$

with the "anharmonicity" coefficients (torsion)

$$a_{hh} = \frac{-1}{16\pi B\rho}\sum_i \pm Q_i\beta_{xi}\alpha_{xi}$$
$$a_{hv} = \frac{1}{16\pi B\rho}\sum_i \pm Q_i(\beta_{xi}\alpha_{yi} - \beta_{yi}\alpha_{xi})$$
$$a_{vv} = \frac{1}{16\pi B\rho}\sum_i \pm Q_i\beta_{yi}\alpha_{yi}$$

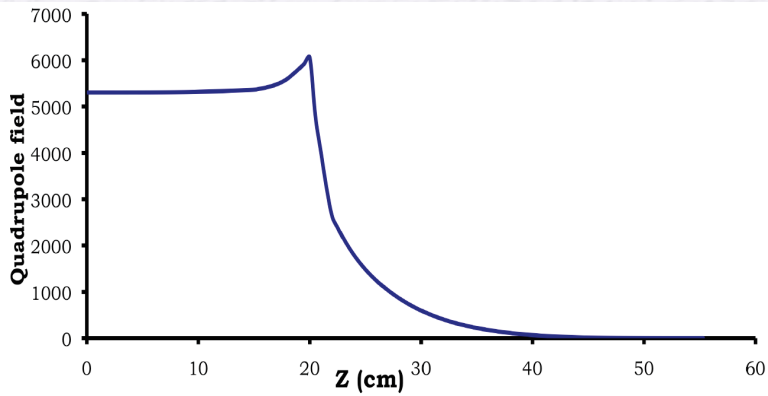


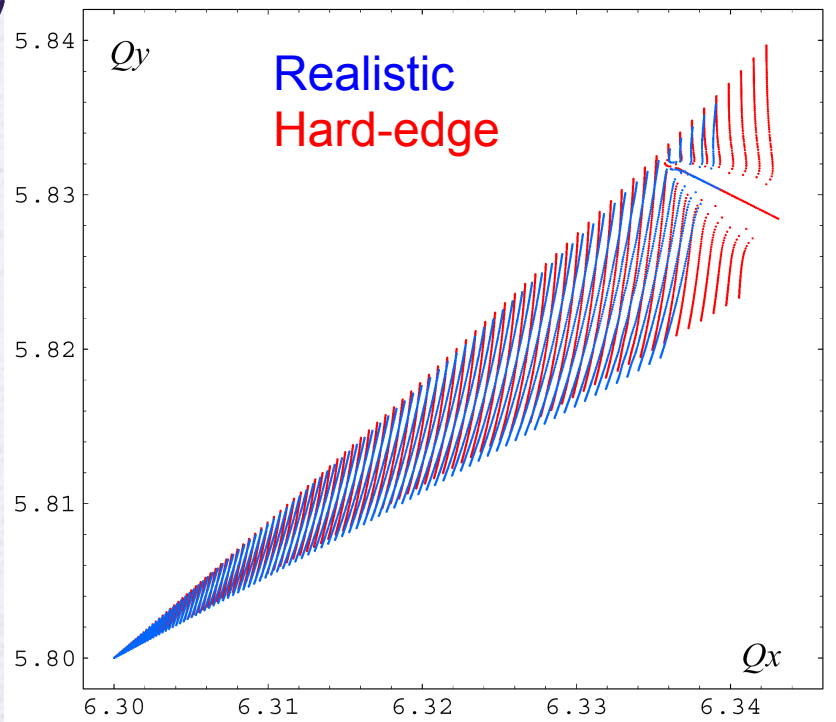

# Off-momentum frequency maps

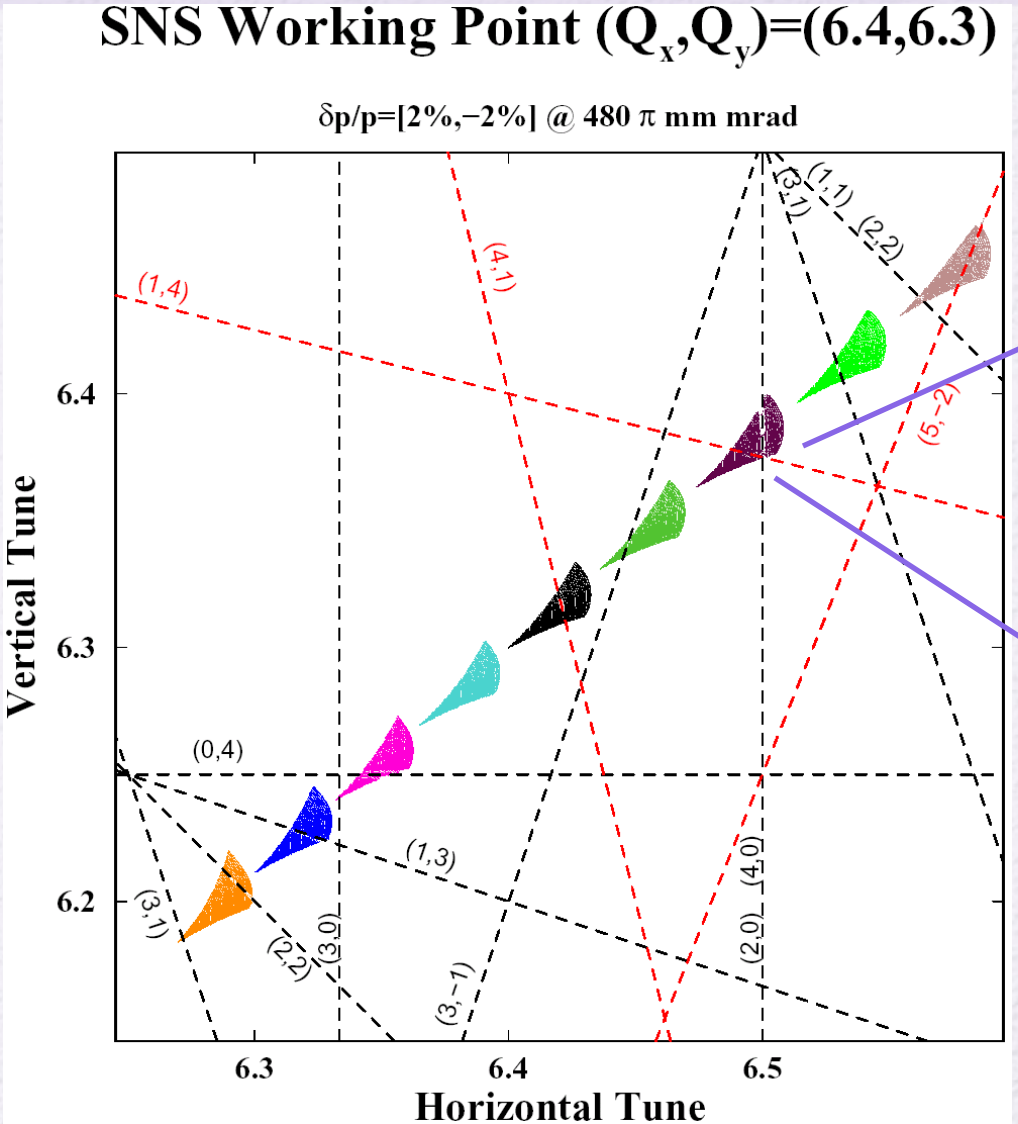


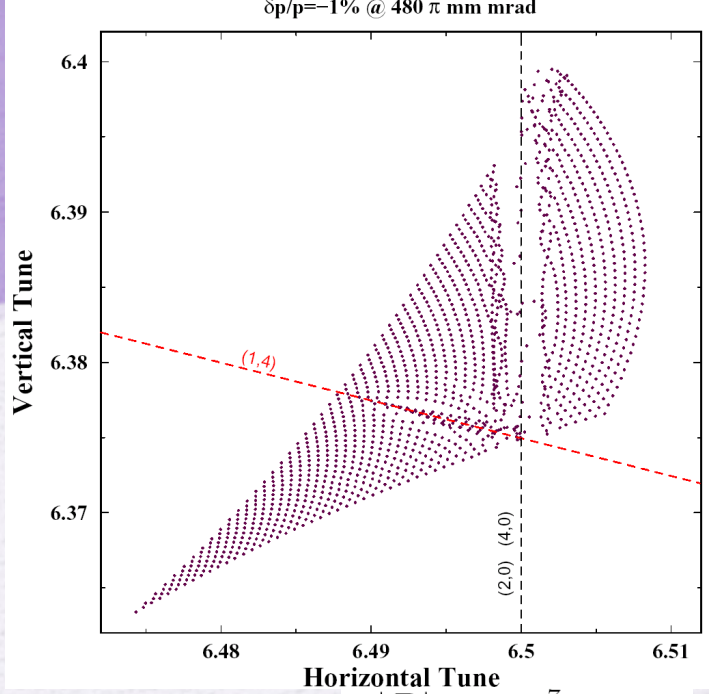


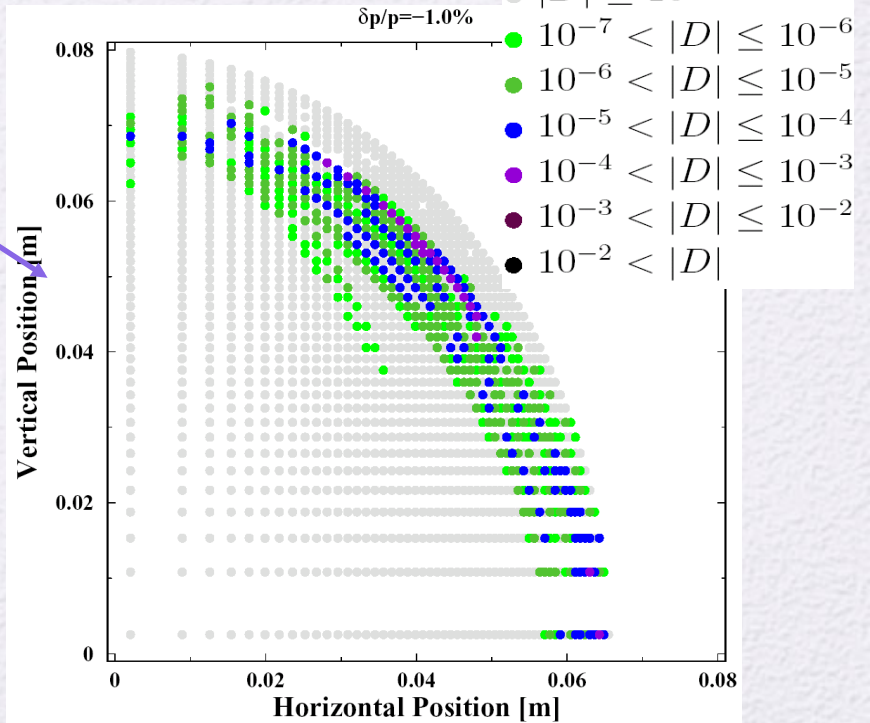

# Choice of the SNS ring working point

Tune Diffusion quality factor

$$D_{QF} = \left\langle \frac{|\boldsymbol{D}|}{(I_{x0}^2 + I_{y0}^2)^{1/2}} \right\rangle_R$$

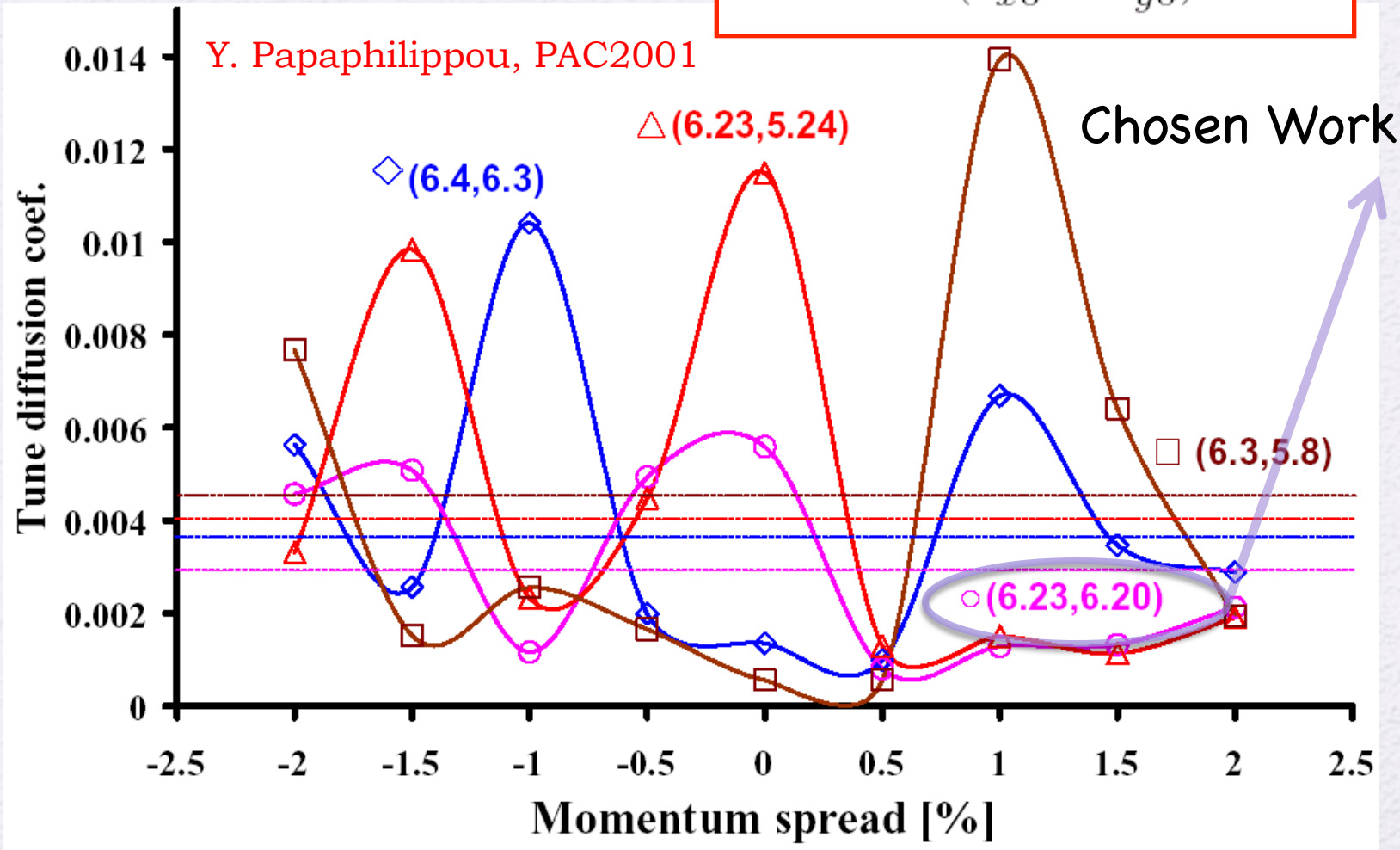

# Working point choice for SUPERB

S. Liuzzo et al., IPAC 2012

- Figure of merit for choosing best working point is sum of diffusion rates with a constant added for every lost particle
- Nominal working point had to be moved towards "blue" area

$$e^D = \sqrt{\frac{(\nu_{x,1} - \nu_{x,2})^2 + (\nu_{y,1} - \nu_{y,2})^2}{N/2}}$$

$$WPS = 0.1 N_{lost} + \sum e^D$$

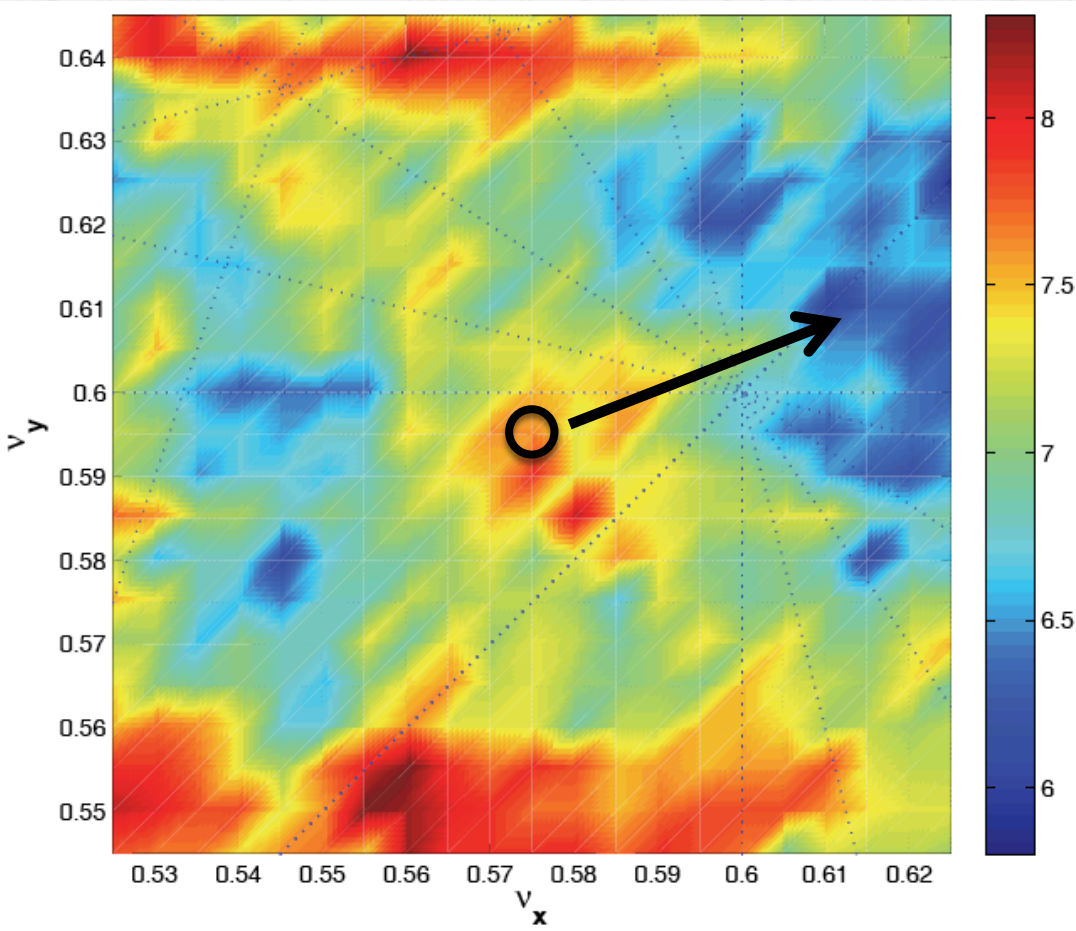

# Beam-Beam interaction

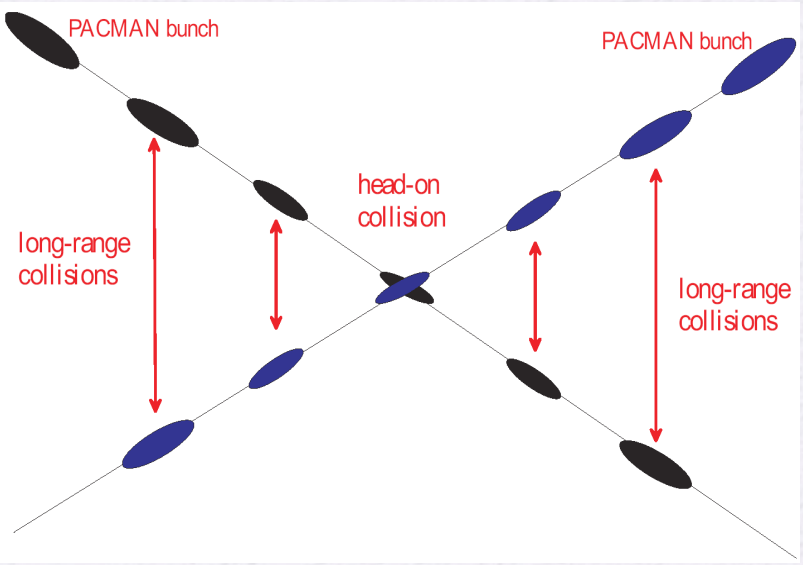


Long range beam-beam interaction represented by a 4D kick-map

$$\Delta x = - n_{par} \frac{2 r_p N_b}{\gamma} \left[ \frac{x' + \theta_c}{\theta_t^2} \left( 1 - e^{- \frac{\theta_t^2}{2\theta_{x,y}^2}} \right) - \frac{1}{\theta_c} \left( 1 - e^{- \frac{\theta_c^2}{2\theta_{x,y}^2}} \right) \right]$$

$$\Delta y = - n_{par} \frac{2 r_p N_b}{\gamma} \frac{y'}{\theta_t^2} \left( 1 - e^{- \frac{\theta_t^2}{2\theta_{x,y}^2}} \right)$$

with $\theta_t \equiv \left( (x' + \theta_c)^2 + y'^2 \right)^{1/2}$

# Head-on vs Long range interaction

Y. P. and F. Zimmermann, PRSTAB 1999, 2002

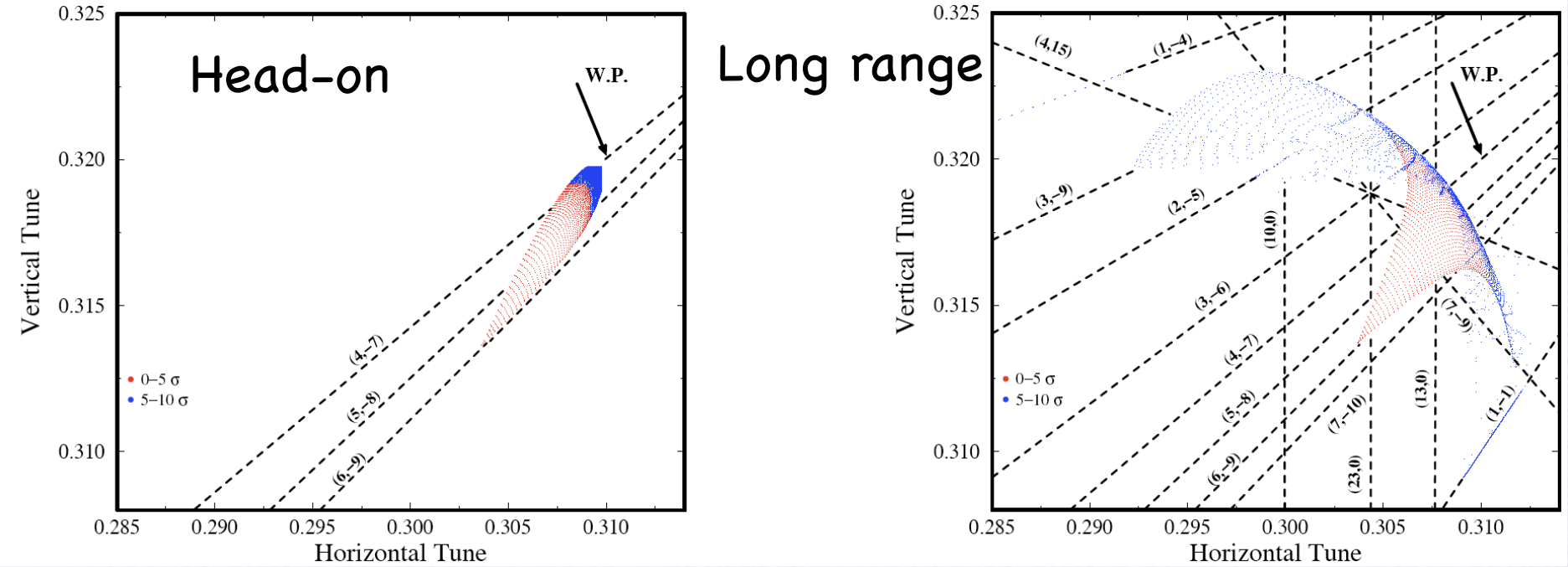


- Proved dominant effect of long range beam-beam effect
- Dynamic Aperture (around 6 $\sigma$) located at the folding of the map (indefinite torsion)
- Dynamics dominated by the 1/r part of the force, reproduced by electrical wire, which was proposed for correcting the effect

# Action variance vs. frequency diffusion coefficient

Y. P. and F. Zimmermann, PRSTAB 1999, 2002

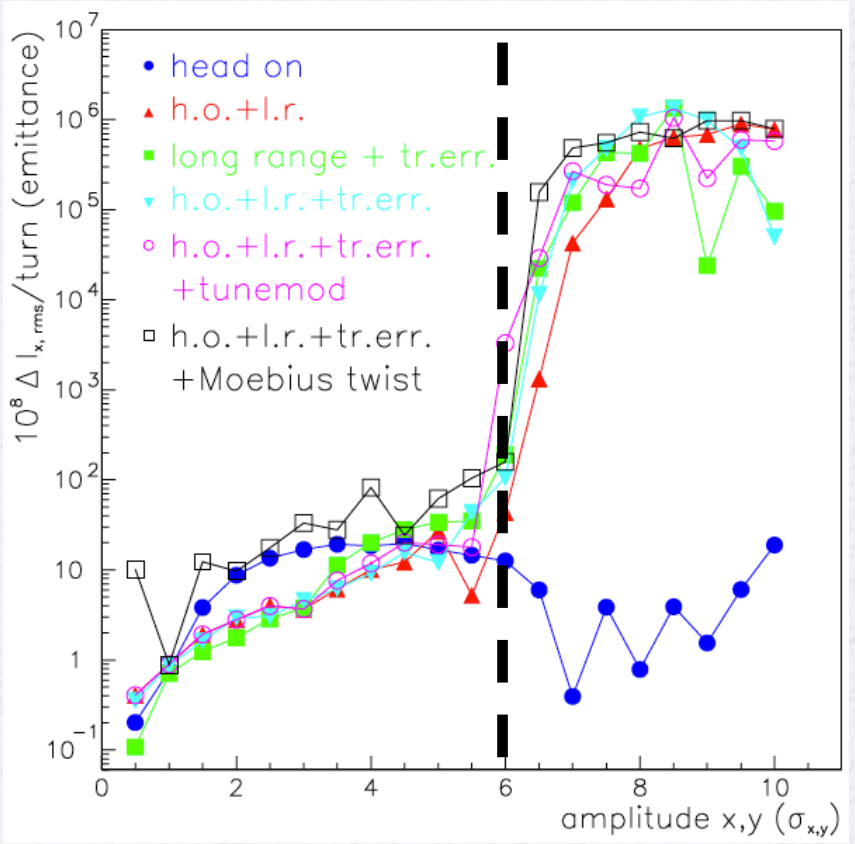


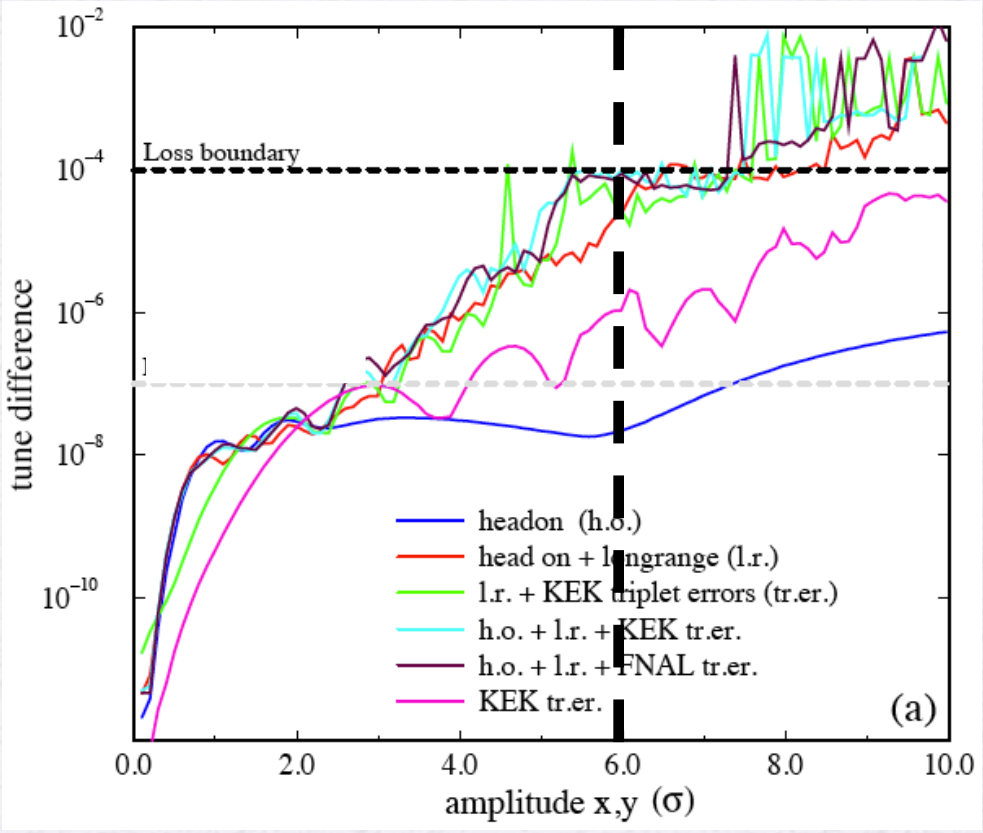


- Very good agreement of diffusive aperture boundary (action variance) with frequency variation (loss boundary corresponding to around 1 frequency unit change in $10^7$ turns)

# CERN PS2 sextupole scheme optimization

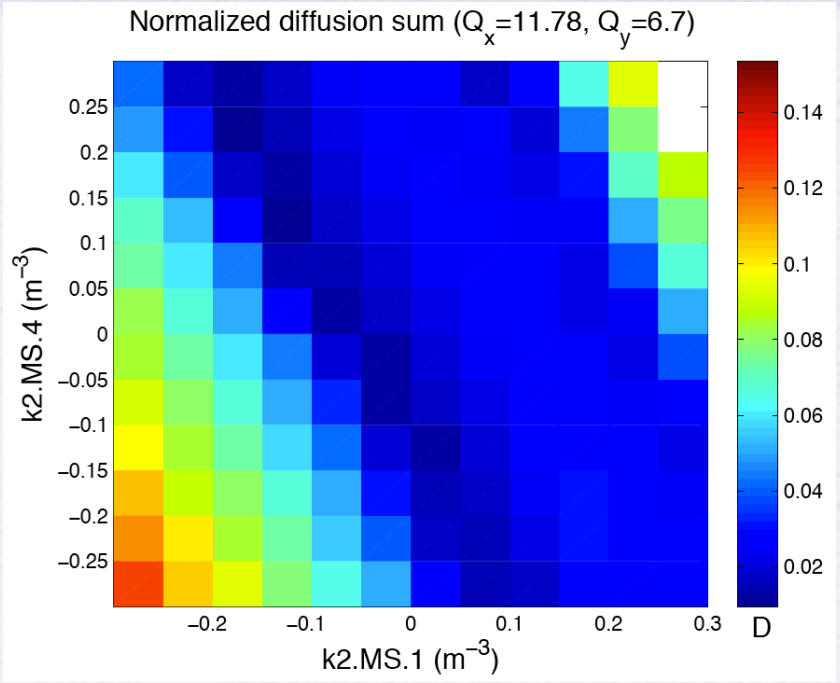


H. Bartosik and Y. P. , HB2010, 2010

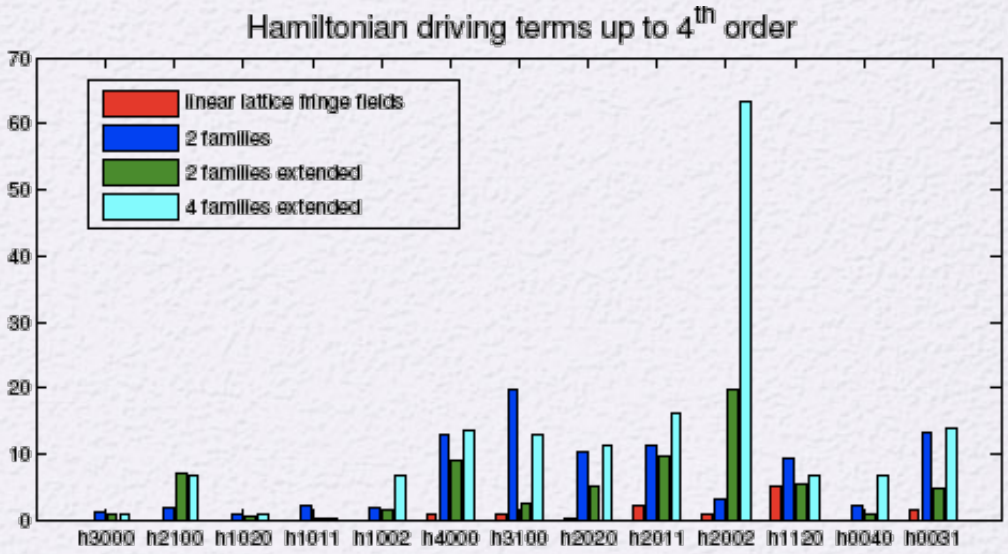


- Comparing different chromaticity sextupole correction schemes and working point optimization using normal form analysis, frequency maps and finally particle tracking
- Finding the adequate sextupole strengths through the tune diffusion coefficient

# Beam loss frequency maps in the SPS

H. Bartosik and Y. P., 2012

- Strength of resonance lines identified by derivative of beam intensity (average beam loss rate)
- Tunes continuously monitored using NAFF and beam intensity recorded with current transformer

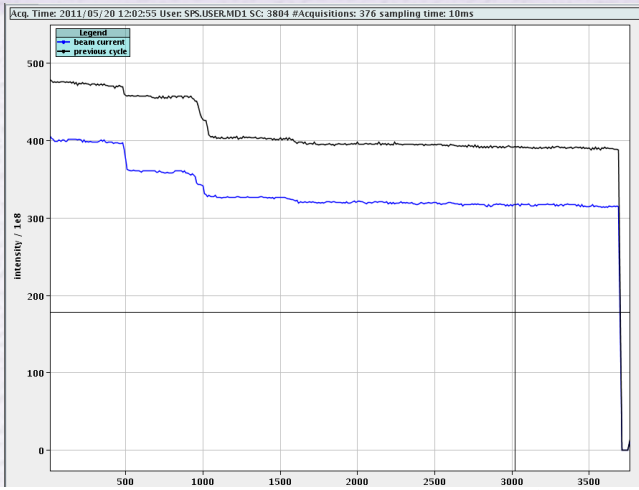


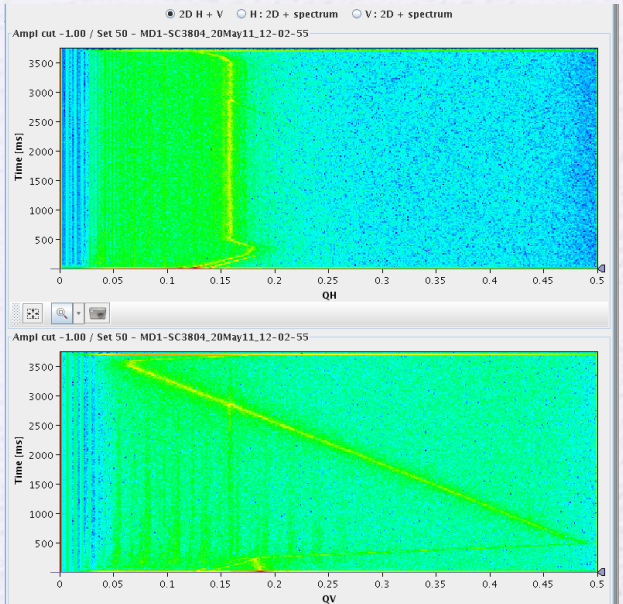


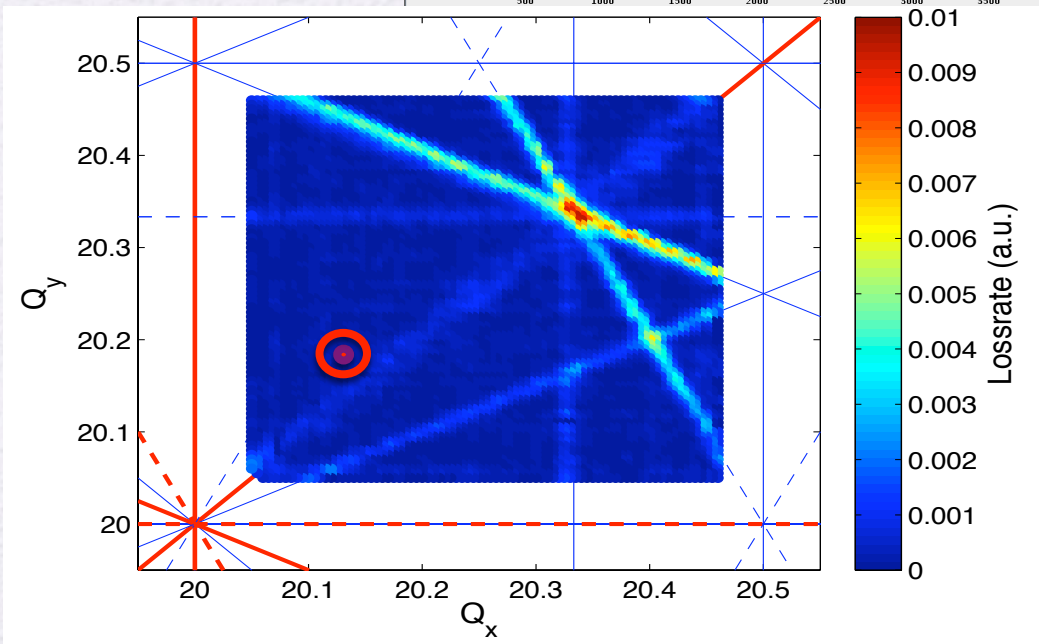

# Summary for beam dynamics


- Study and correction of non-linear effects crucial for the design and performance optimization of particle accelerators
- Non-linear dynamical system methods are fundamental in order to achieve this task
- The application of the frequency map analysis has become a necessary step for understanding and optimizing the dynamics of accelerator models
- Its application to experimental data gives tremendous insight regarding the dynamic behavior of an operating accelerator

# Special thanks and wishes


I would like to thank J. Laskar for the tremendous impact his early mentoring had to my scientific career